2012

Development of a Novel Lateral-Flow Assay to Detect Yeast Nucleic Acid Sequences

Catherine E. Fill
University of Massachusetts Amherst

DEVELOPMENT OF A NOVEL LATERAL-FLOW ASSAY TO DETECT YEAST NUCLEIC ACID SEQUENCES

A Thesis Presented

by

CATHERINE E. FILL

Submitted to the Graduate School of the

University of Massachusetts Amherst in partial fulfillment

of the requirements for the degree of

MASTER OF SCIENCE

May 2012

Department of Food Science

DEVELOPMENT OF A NOVEL LATERAL-FLOW ASSAY TO DETECT YEAST NUCLEIC ACID SEQUENCES

A Thesis Presented

By

CATHERINE E. FILL

Approved as to style and content by:

.....
Sam R. Nugen, Chair

.....
Julie M. Goddard, Member

.....
Lynne A. McLandsborough, Member

.....
Eric A. Decker, Department Head
Food Science

ACKNOWLEDGEMENTS

I would like to thank Dr. Sam Nugen for his guidance and mentoring throughout my master's program. My lab mates, especially Yuhong Wang, Faye He, and Shengquan Jin, were incredibly helpful and supportive during the tough times. All the friends I made in the department were wonderfully encouraging. Thank you for all the lunches in the break room and hallway conversations. They always made a huge improvement in my day.

ABSTRACT

DEVELOPMENT OF A NOVEL LATERAL-FLOW ASSAY TO DETECT YEAST IN YOGURT

MAY 2012

CATHERINE E. FILL, B.S., BUFFALO STATE COLLEGE

M.S., UNIVERSITY OF MASSACHUSETTS AMHERST

Directed by: Professor Sam R. Nugen

As demand for food increases, rapid testing methods are becoming increasingly important. In the past few years, yogurt has become very popular. Yeast species are the most common spoilage organism that cost consumers and food companies money. A novel lateral flow assay has been developed to detect yeast oligonucleotide sequences. Gold nanoparticles were used as the standard reporter and fluorescent nanoparticles were developed as the novel reporter. Specifically, the fluorescent nanoparticles were ruthenium-doped silica nanoparticles synthesized using the modified Stöber method. Visual analysis of the assays using gold nanoparticle reporters showed the limit of detection to be 10 femtomoles of target sequence. Analysis of the fluorescent nanoparticles using a plate reader showed the limit of detection to be 0.027 femtomoles. The fluorescent reporter's limit of detection is 1000 fold lower due to a more sensitive and sophisticated analysis method. Gold nanoparticles are appropriate for presence or absence testing, but fluorescent nanoparticles are best for obtaining quantitative data with low detection limits.

Pathogens have been used as biological warfare for centuries. Since the terrorist attacks of 2001, awareness of biowarfare agents has increased. A brief review of

common biowarfare agents is included. *Yersinia pestis*, the causative agent of the Plague, and *Bacillus anthracis*, the causative agent of Anthrax, are the focus. They are both considered classical agents of biological warfare. After *B. anthracis* spores were sent through the mail in 2001, increased research has gone into improved detection methods and decontamination processes.

Gold nanoparticles were also used as a reporter in a sandwich assay to detect *E. coli*-like sequences with the Bioveris M384 Analyzer. This reporter had several molecules of $Ru(bpy)_3^{2+}$ immobilized on the surface. It was compared to a control reporter, which was an oligonucleotide strand linked to a single ruthenium. The hypothesis was that the novel reporter would have a higher sensitivity and lower limit of detection than the control. Repeated testing showed the novel reporter had a limit of detection 24 femtomoles compared to the control's 40 femtomoles. This improvement is due to the novel reporter's ability to bind more target than the control reporter.

TABLE OF CONTENTS

Page

LIST OF TABLES

LIST OF FIGURES

LIST OF ABBREVIATIONS

CFU ..... Colony Forming Unit

MPN ..... Most Probable Number

GNP ..... Gold nanoparticle

NC ..... Nitrocellulose

W/O ..... Water in oil (emulsion)

TEM ..... Transmission Electron Microscopy

fmol ..... Femtomoles (10^{-12})

$Ru(bpy)_3^{2+}$ ..... Tris(2,2'-bipyridyl)ruthenium(II)

rRNA ..... Ribosomal ribonucleic acid

PBS ..... Phosphate buffered saline

TBS ..... Tris-buffered saline

BSA ..... Bovine serum albumin

OD ..... Optical density

SiNP ..... Silica nanoparticle

SSC ..... Saline-sodium citrate

B&W ..... Binding and Washing Buffer

CHAPTER 1

STUDY OVERVIEW AND BACKGROUND INFORMATION

Introduction

Yogurt and yogurt based products are becoming increasingly popular due to health benefits, expanded product lines, taste, and nutritional value. Increased production leads to an increased possibility of contamination by spoilage organisms, specifically yeast. Traditional microbiological tests take several days before results are returned. Therefore, a rapid lateral-flow based test to detect Eukaryotic spoilage organisms in yogurt has been developed.

Yogurt and possible contaminants

Yogurt is a fermented milk product with a low pH due to the production of lactic acid by the fermenting starter cultures. Yeasts thrive in dairy products because of the acidic, nutrient rich environment (Jakobsen and Narvhus, 1996). These spoilage organisms are capable of fermenting lactose, producing extracellular proteolytic or lipolytic enzymes, or assimilating lactic and citric acids (Kosse *et al*, 1997). As the yeast population increases, the bacterial population decreases from the lack of nutrient availability and decreasing pH. Contamination sources include fruits, nuts, honey, and other raw products that are added to the yogurt, as well as dairy products, intermediate products, the environment, and poor plant sanitation or hygiene. These additives provide additional substrates for the yeast (Jakobsen and Narvhus, 1996; Fleet, 2011; Mataragas *et al*, 2011).

Species of yeast that are common contaminants in yogurt and dairy products include *Saccharomyces cerevisiae*, *Kluyveromyces marxianus*, and species of *Pichia* and *Candida* (Fleet, 2011). Some of the species can grow at refrigeration temperatures, resist preservatives, and tolerate high sugar or high salt environments. Yogurt spoilage is detectable through analytical methods when growth reaches 10^4-10^6 colony forming unit per gram (CFU/g) and evident through sensory evaluation when populations reach 10^7-10^8 CFU/g (Fleet, 2011; Viljoen *et al*, 2003). Spoilage includes package distortion, yeasty flavor and odor, gassy appearance, and red colony growth (Viljoen et al, 2003; Fleet, 2011; Mataragas *et al*, 2011). Yeast populations increase with increasing temperature (Viljoen *et al*, 2003; Mataragas *et al*, 2011). The product can be re-contaminated with environmental yeast following heat treatment due to increased automation in the production facility (Nugen and Baeumner, 2008). The batch of yogurt may have been contaminated after the sample was taken for testing. In this case, the test results would falsely state the batch does not have a detectable presence of yeast. Therefore, spoilage is likely to be a concern after it has left the production facility due to temperature abuse by the retailer or consumer.

Enumeration and detection methods- current and proposed

The isolation, enumeration, and identification of yeasts using traditional microbiological methods are most often used in the food industry. Traditional methods based on biochemical, physiological, and morphological differences have been peer reviewed and are most accepted by regulatory agencies. They are also considered open access methods, meaning media composition is available, the techniques used are clearly described to reproduce data, and the necessary materials can be purchased from several

suppliers (Jasson *et al*, 2010). These processes are labor intensive and time consuming since it may take days to weeks to obtain and confirm results (Velusamy *et al*, 2010). After initial positive results are obtained, similar species of yeast may be difficult to distinguish (Kosse et al, 1997). The materials used must be properly disposed of after the results have been obtained. The yogurt samples must be washed and diluted before enumeration via spread plate, most probable number (MPN), microscopic, or other counting methods. Isolates must then be purified before the genus, species, and subspecies can be determined. Spread-plate methods are used to enumerate and isolate yeast. A minimum of five days of incubation is required to develop colonies (Jakobsen and Narvhus, 1996). Traditional methods are very selective and frequently do not provide a complete picture of the entire, complex microbial community present in the sample (Amann and Ludwig, 2000). Alternative methods that provide results in hours instead of days are needed. Methods that provide more complete information about the microbial population would also be useful to detect more than one target organism with one assay. In order for these alternative methods to be accepted, they must the validated by a third party against the traditional method (Jasson *et al*, 2010).

Lateral-flow tests are rapid, easy to use, specific, and robust (Al-Yousif *et al*, 2002). A lateral-flow test using sandwich hybridization to detect sequences of yeast DNA, similar to those found in yogurt has been developed. Nucleic acid sequences were used as the detection elements and gold or fluorescent nanoparticles were used as the reporter element. The surface of the nanoparticle was modified to facilitate the addition of a reporter sequence. A schematic drawing of the test is shown in Figure 1.1.

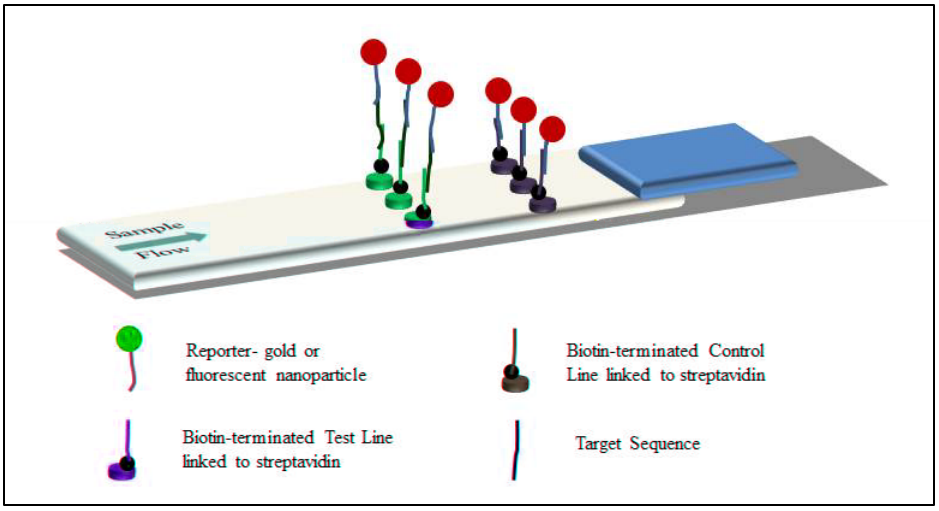

Figure 1.1- Schematic drawing of the novel lateral-flow test strip. The reporter nanoparticle is represented by the red circle with blue reporter sequence. The test and control line areas are symbolized by the green and purple cylinder and nucleic acid sequence, respectively. Biotin is symbolized by the black dot. The target sequence is symbilized by the dark green line. The absorbent pad is blue and the plastic backing is grey.

A liquid sample is needed for testing and results are obtained within 15-30 minutes. Gold nanoparticle (GNP) reporter results can be seen with the naked eye. Tests using the fluorescent nanoparticles are read in a plate reader and more quantitative data is obtained. The lines that develop are long lasting, so the test can be evaluated at the user's convenience. The tests are easily transportable and do not require special training or equipment. Ease of use facilitates near on-line detection in a production facility.

CHAPTER 2

REVIEW OF LATERAL-FLOW TECHNOLOGY AND NANOPARTICLE DESIGN

Introduction

Rapid testing methods are becoming increasingly popular in the health care and private sector. Lateral-flow assays are very popular. The most well-known and well-recognized example is the home pregnancy test. It is used to detect human chorionic gonadotropin (hCG), a chemical marker associated with pregnancy (Butler *et al*, 2001). The test's ease of use and rapid, clear results lead to an expansion of uses in the clinical and industrial settings. Lateral-flow assays are used to detect failure of internal organs (Xu *et al*, 2009), contamination or infection with a specific pathogen (Yan *et al*, 2006; Oku *et al*, 2001; Esch *et al*, 2001), presence of toxins in food or environmental samples (Wang *et al*, 2005; Rong-Hwa *et al*, 2010; Muhammad-Tahir and Alocilja, 2004; Yang *et al*, 2009; Gessler *et al*, 2007), or to detect the use of illegal drugs (Biermann *et al*, 2004; Posthuma-Trumpie *et al*, 2009). The lateral-flow format of testing is primarily used for presence or absence testing because it is hard to relate strength of the test line with target concentration without specialized equipment.

Lateral Flow Components

A typical lateral flow assay is shown in Figure 2.1. The test strip is housed in a plastic cassette that allows for easy handling, transportation, and evaluation of results. The liquid sample is applied to the sample pad that is visible through the sample window. The sample pad (Fig 2.1A) can be made of cellulose or glass fiber. It is used to filter out

unwanted components in the sample that may interfere with the results and to evenly distribute the sample to the next part of the assay (Leung *et al*, 2003). The sample pad is overlapped by the conjugate pad (Fig 2.1B), which can be made of fiberglass, polyester, or synthetic, non-absorbent material (Koets *et al*, 2006). The conjugate pad contains the dried reporter conjugate (Fig 2.1C), which is seen by the user in the viewing window as a colored line. It is bound to a biorecognition element, such as an antibody or nucleic acid fragment, that will interact with the target in the sample or with the control line. The most common reporters are gold nanoparticles (GNPs) and colored latex particles, but carbon particles or fluorescent particles can be used as well (Posthuma-Trumpie *et al*, 2009). Particle stability is most important when selecting a reporter material.

The reaction chamber (Fig 2.1D) in this assay is typically made of nitrocellulose (NC) due to its low cost, ease of use, and its ability to support capillary flow. The pore size of the membrane plays a major role in the performance of the assay. Large pores will decrease the sensitivity of the assay because the test line will spread out and be difficult to read (Posthuma-Trumpie *et al*, 2009). The pore size also dictates the flow rate of the reporter and target. If the pores are too small, passage will be restricted. The test and control lines (Fig 2.1E and F, respectively) give the user the test results. The test line interacts with the target-reporter complex. A visible line of the reporter conjugate appears if the target is present in the sample. The control line interacts with the reporter conjugate to verify the sample is flowing up the NC and the reporter conjugate is working properly. The test and control line can be applied to the NC in many different ways. The recognition elements on the test and control lines and reporter conjugate are either antibodies or nucleic acids. Nucleic acid recognition elements will be focused on in this

literature review and will be used in the subsequent experiments. The absorbent pad (Fig 2.1G) is used to help draw the sample up the NC once it has been fully saturated with liquid. It is typically made of cotton and varying thicknesses have different absorbency rates (Posthuma-Trumpie *et al*, 2009). The strip is assembled on plastic backing (Fig 2.1H) which gives the assay strength and rigidity.

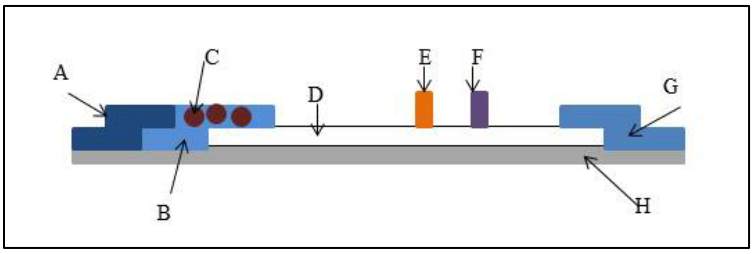

Figure 2.1- Schematic representation of a lateral-flow test strip in sandwich format. 2.1A is the sample pad, 2.1B is the conjugate pad, 2.1C is the dried reporter conjugate, 2.1D is the nitrocellulose membrane, 2.1E and F are the test and control lines, respectively, 2.1G is the absorbent pad, and 2.1H is the plastic backing. The test strip is protected by a plastic cassette. The beginning of the sample pad and the test and control line area are left exposed for the user to apply the liquid sample and view the test result.

Lateral flow assays are available in a variety of formats. They can be set up in a sandwich or competitive format. In the sandwich format, the target is "sandwiched" between the test line and reporter conjugate. The intensity of the test line is directly proportional to the target concentration (Volkov *et al*, 2009). Two lines indicate a positive test and one line indicates a negative test. This format is very common (Al-Yousif *et al*, 2002; Koets *et al*, 2006)). In the competitive format, the target and reporter conjugate compete for open binding spots on the test line (Esch *et al*, 2001; Volkov *et al*, 2009). The reporter conjugate is pre-labeled with the target or target derivative. A positive sample does not show a test line because the target in the sample binds to the test line before the reporter conjugate. A negative sample shows a test line because the

reporter conjugate is able to bind to the reaction zone. Therefore, signal strength is inversely proportional to the target concentration.

Fluorescent nanoparticles

Stöber and colleagues (1968) were the first to synthesize monodisperse silica particles. This was achieved by combining alcohol, water, and alkyl silicate under alkaline conditions. The reaction vessel was agitated, which helped the particles to form and keep them suspended. It was reported that condensation began in about ten minutes due to the increased turbidity of the once clear solution. The reaction went to completion in a few minutes after the solution turned milky white. Electron micrograph evaluations of the particles revealed a monodisperse solution of silica particles. The size of the particles and rate of synthesis was related to the type of alcohol and type of alkyl silicate used.

Since its initial development, the Stöber method has become a common way to synthesize nanoparticles (Rossi *et al*, 2005; Santra *et al*, 2001b, Smith *et al*, 2006). The "modified Stöber method" is often used because it is an easy, one pot method to make dye-doped silica nanoparticles. A water-in-oil (W/O) emulsion is first formed. The water phase serves as a nanoreactor and contains the dye. It is surrounded by surfactants to improve solubility. Silica is condensed around the water phase. The reaction is allowed to continue for a set reaction time depending on the desired size of the particles. The size of the particles is determined by the nanoreactor size, volume of dye loaded into the nanoreactor, and incubation time. Figure 2.2 shows a typical W/O emulsion.

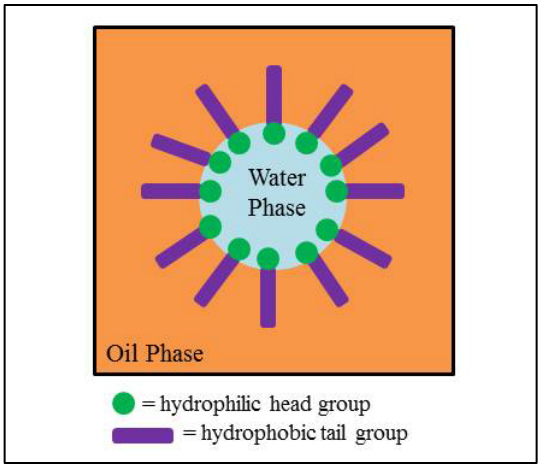

Figure 2.2- Schematic drawing of a typical water in oil (W/O) emulsion. The surfactant molecule is represented by the green circle and purple rectangle. The green circle represents the hydrophilic head group which surrounds the water phase and the purple rectangle represents the hydrophilic tail group which interacts with the surrounding oil phase. Surfactants are able to stabilize immiscible liquids because of their hydrophilic and hydrophobic natures.

Surfactant molecules have a polar head group and non-polar tail. The polar end is attracted to the polar water phase while the non-polar end interacts with the surfactants located in the non-polar oil phase and the dye is dissolved in the water phase. After the emulsion is formed, the catalyst and silica reagent are added. Silica layers condense around the water phase to trap the dye and form a nanoparticle (Ow *et al*, 2004). The size of the particles is dependent upon reaction time and volume of materials added. Nanoparticles are typically imaged with transmission electron microscopy (TEM).

Fluorescent nanoparticles have great potential for use in biotechnological applications as indicators or photon sources or in information technology applications as biological imaging, sensor technology, microarrays, and optical computing (Ow *et al*, 2004). Fluorophores such as organic dyes are used to detect biological components in living systems, but their use has some limitation. Photobleaching decreases sensitivity and limits real-time monitoring (Santra *et al*, 2001a). Poor signal amplification can lead to false negative results. The component of interest may only be tagged with one or two

dye molecules and the signal may be undetectable when target concentration is low (Zhao *et al*, 2003).

One way to overcome these hurdles is to use fluorescent nanoparticles. The silica shell surrounds the dye and prevents leakage. This "caging effect" also limits the dye's contact with environmental oxygen and solvents, thus improving the dye's photostability (Rossi *et al*, 2005). The silica encased dye molecules have been reported to be several times brighter than free dye because a high concentration of dye molecules are trapped in the nanoparticles (Ow *et al*, 2005). A high signal is produced when the particle is excited properly. Now instead of one dye molecule labeling one target molecule, one nanoparticle containing dozens of fluorophores labels the target and a detectable signal is produced (Zhao *et al*, 2003). Photobleaching experiments show the fluorescent nanoparticles are brighter and more stable than the free dye (Smith *et al*, 2006; Zhao *et al*, 2003). The surface of the nanoparticle can also be easily modified using surface chemistry. Surface modification allows for the addition of antibodies, nucleic acid sequences, or other recognition elements depending on the intended target.

Biomolecules can be covalently linked to the nanoparticle for use in biological systems. The silica surface is a biocompatible and versatile substrate. Santra and colleagues (2001b) were able to link anti-leukemia cell antibodies to the doped nanoparticle and detect cancer cells. Zhao and colleagues (2003) linked DNA sequences to their nanoparticles and detected target sequences at sub-femtomolar (10^{-12}) concentration.

Many different dyes can be doped into the silica matrix depending on the desired spectral characteristics and color of the end product. Ruthenium is a transition metal that

exists in many forms and is a common fluorophore. Tris(2,2'-bipyridyl)ruthenium(II), $Ru(bpy)_3^{2+}$, is attractive because it is stable, bright, and can regenerate itself (Chang *et al*, 2006). The chemical structure contains several double bonds. $Ru(bpy)_3^{2+}$ was chosen for this project because it is stable, rapid, safe to use, and emits light at the desired wavelength (620 nm).

Probe selection and design

Selecting the correct probe is crucial for the success of an assay. Nucleic acid probes are precise and can offer a quantitative description of the total microbial population of a sample (Kuritza and Salyers, 1985; Giovannoni *et al*, 1985; Amann and Ludwig, 2000). The reporter probe must match perfectly to its target. Even a single mismatch can destabilize an oligonucleotide hybrid (Giovannoni *et al*, 1988; Amann *et al*, 1990). Targeting a nucleic acid probe to ribosomal RNA (rRNA), specifically to the 16S or 18S region of the small ribosomal subunit, is a good way to analyze the microbial population. There is a large amount of rRNA present in most cells, there is no lateral gene transfer, the small and large subunits have 1500-3000 nucleotides, and there is a range of conserved and variable regions (Amann and Ludwig, 2000; Woese, 1987). Actively growing cells can have 10^4 ribosomes. With each ribosome acting as a probe target, it is possible to label and identify a single microbe (Giovannoni *et al*, 1988). rRNA databases are helpful for comparative analysis of sequences.

When comparing the genetic material of two or more organisms, the regions of the DNA or RNA can be conserved or variable. Conserved regions are sequences of nucleic acids that are similar or nearly identical across species (Lane *et al*, 1985; Giovannoni *et al*, 1988). By targeting conserved regions of rRNA, "universal" probes

can be used to detect groups or kingdoms of organisms (Lischewski *et al*, 1996; Amann *et al*, 1990). Universal probes are also useful in detecting the total rRNA content of a sample. Microorganisms can be classified based on differences in their rRNA (Woese, 1987). Probes targeting these variable sequences can help identify an organism. When designing a probe, it is important to select a target region that is easily accessible (Inácio *et al*, 2003; Fuchs *et al*, 1998; Fuchs *et al*, 2001).

EUK516 (5'-ACCAGACTTGCCCTCC) was chosen as the reporter sequence in this experiment. This is a universal Eukaryote probe targeting the 18S rRNA and would be able to hybridize to any Eukaryotic organism in the sample, giving a more complete estimate of contamination. It was initially used by Amann and colleagues in 1990 as a universal probe to detect Eukaryotes in a mixed microbial population. The number 516 refers to the corresponding position on the *E. coli* 16S rRNA.

After its discovery, this probe was used in several flow cytometric experiments as a control for yeast species (Inácio *et al*, 2003; Lischewski *et al*, 1996) and Eukaryotic organisms (Amann *et al*, 1990). Kosse and colleagues (1997) used 18S rRNA-targeted oligonucleotide probes to identify yogurt spoiling yeasts. Several species specific probes and the universal EUK516 probe were used to detect whole cells using fluorescent in situ hybridization (FISH) and using in situ hybridization to detect yeast inoculated into commercial yogurt. All yeast species were detected by EUK516. Its detection limit of *S. cerevisiae* in yogurt was 10^3 CFU/g. These findings are significant because yeast spoilage of yogurt becomes detectable to the consumer at 10^4-10^6 CFU/g (Fleet, 2011; Viljoen *et al*, 2003). The assay was able to detect spoiled before the consumer could taste it.

EUK1209 (5'-GGGCATCACAGACCTG) was used as the test line sequence. This is another universal Eukaryotic probe that targets the 16S rRNA. Again, the number 1209 refers to the corresponding position on the *E. coli* 16S rRNA. This probe was developed by Giovannoni and colleagues in 1988 while developing phylogenetic group-specific probes to identify single microbial cells in a mixed population. Since its development, this probe has been used as a general Eukaryote probe (Biegala *et al*, 2005). Bochdansky and Huang (2010) used the two most common Eukaryotic probes, EUK516 and EUK1209, to design a new probe specific for a branch of Eukaryotes called Kinetoplastida.

EUK516 Complement (5'-GGAGGGCAAGTCTGGT) was used as the control line because it would hybridize to the control sequence attached to the reporter probe and immobilize it in the reaction zone on the nitrocellulose. The target sequence is a combination of EUK516 Complement and EUK1209 Complement separated by a poly-A spacer. This sequence was designed by the author to prove that the novel system worked and could detect Yeast-like sequences in solution. The reporter probe would be able to hybridize to the EUK516 Complement and the test line would be able to hybridize to the EUK1209 Complement, completing the sandwich style assay in the reaction zone.

Once the nanoparticle reporters were synthesized, the reporter probe needed to be immobilized on the surface. The test line sequence also needed to be immobilized on the nitrocellulose test strip. The biotin-streptavidin link is the strongest non-covalent bond (Nobs *et al*, 2004). This was used to anchor the reporter probe to the nanoparticle. The surface was first coated with avidin. The reporter probe was purchased premodified with biotin. It was bound to the avidin on the surface of the reporter resulting in a nucleic acid

tagged nanoparticle. The biotin-avidin link was also used to immobilize the test and control lines to the nitrocellulose (Edwards and Baeumner, 2006). Avidin easily adsorbs to nitrocellulose.

The fluorescent particles were prepared using covalent immobilization. Aminosilanes were first added to the silica surface. The terminal amino group was activated by glutaraldehyde. The amino-terminated reporter sequence was then permanently immobilized on the surface via the covalent bond between the amino group on the reporter probe and the aldehyde (Zhang *et al*, 2009; Nobs *et al*, 2004; Vandenberg *et al*, 1991; Howarter *et al*, 2006)

CHAPTER 3

COMPARISON OF GOLD NANOPARTICLES TO FLUORESCENT NANOPARTICLES AS A REPORTER IN A LATERAL-FLOW ASSAY

Research design and rationale

The nucleic acid sequences were chosen based upon the literature. These sequences are probes used for detection of yeast and other Eukaryotic organisms. The target sequence is complementary to both the test line and reporter sequence. The reporter sequence is complementary to the control sequence. Two different reporter conjugates were used. Gold nanoparticles are the accepted standard and are used in commercial products. A novel fluorescent nanoparticle was developed to gain more qualitative data from the assay. Nitrocellulose was used as the reaction chamber of the assay and was treated to allow for optimal movement of the nanoparticle reporters.

Test strip preparation

Nitrocellulose selection and preparation

The nitrocellulose (NC) reaction chamber was prepared first. AE98 (GE Whatman) was cut to a width of 38 mm using a paper cutter. Double-sided transfer tape (3M) was used to anchor the NC to the plastic backing. Plastic sheets cut to a width of 75mm were used to provide strength and rigidity to the test strip. The tape was placed 10mm from the bottom of the plastic. This left about 27 mm for the application of an absorbent pad. After the NC was added, the assembly was kept in a desiccating chamber until needed.

Test and control line application

All test and control line sequences were purchased with a biotin modification from Eurofins MWG Operon (Huntsville, AL). All sequences used are listed in Table 3.1. They were shipped as a lyophilized powder and were reconstituted to 300 μM with PBS buffer (phosphate buffered saline, pH 7.4; 8 g NaCl, 0.2 g KCl, 1.44 g Na_2HPO_4, 0.24 g KH_2PO_4 (Fisher Scientific,)) upon arrival, separated into aliquots, and stored at -4°C until needed.

Table 3.1. List of Yeast sequences used in the proceeding experiments.

Sequence Name	**5'-3' Sequence**	**Reference**	**Common Sequence Name**
Biotin-terminated reporter	Biotin-ACCAGACTTGCCCTCC	Amann *et al*, 1990	EUK516
Amine-terminated reporter	Amine- ACCAGACTTGCCCTCC	Amann *et al*, 1990	EUK516
Test Line	GGGCATCACAGACCTG-Biotin	Giovannoni *et al*, 1988	EUK1209
Control Line	Biotin-GGAGGGCAAGTCTGGT		EUK516 Complement
Target	CAGGTCTGTGATGCCCAAAAAA AAAAAGGAGGGCAAGTCTGGT		EUK516 Complement + EUK1209 Complement

To finish preparing the NC, the control sequence was thawed. Ten microliters of the stock control line sequence was mixed with 10 μL of 95nmol streptavidin (SouthernBiotech, Birmingham, AL) and 30 μL of a buffer containing 0.4M $NaHCO_3/Na_2HCO_3$, pH 9.0, containing 5% methanol (Edwards and Baeumner, 2006). The three components were mixed in a small tube and incubated for 20 minutes. While the control line sequence was incubating, the same procedure was repeated using the test line sequence. After incubation, the control line mixture was drawn into a syringe and

applied to the NC using a Linomat IV (Camag, Wilmington, NC) approximately 28mm from the bottom of the NC. The test line was applied in the same manner four millimeters below the test line. The membrane was dried in a vacuum oven at 40°C at 15" HG for 90 minutes. It was then left overnight in a desiccating chamber before further treatment.

Blocking

After the completed application of the test and control lines, the NC must be blocked with protein to prevent the nanoparticle reporters from adsorbing to the surface. A blocking solution was made using 0.15% casein (MP Biomedicals, Ohio), 2% (w/v) polyvinylpyrrolidone (PVP; size K16-18; Acros Organics), 5% Tween 20 (Fisher Bioreagents), and 10X Tris-buffered saline (TBS; 200mM Tris, 1.37 M NaCl, 1% BSA) (Edwards and Baeumner, 2006). The membranes were first cut into smaller, more manageable pieces and then blocked by placing the plastic backed membranes into the solution with the membrane side down and gently swirled for one minute. Excess solution was blotted off and the membranes were dried in a vacuum oven at 25-30°C at 15" Hg for 2-3 hours. The blocked membranes were kept in a desiccating chamber until needed.

Lateral flow strip assembly

After blocking, the membrane was cut into 4 mm wide strips using a paper cutter. The absorbent pad (CF5; GE Whatman) was added to the NC strip using transfer tape. The CF5 absorbent pad was first cut into pieces measuring 4 x 25 mm. It overlapped the NC by about 2 mm. The assembled lateral flow strips were kept covered in the desiccating chamber until needed.

Reporter preparation

The reporter is the visual aide that relays the test results to the user. Gold nanoparticles (GNPs) are considered to be the standard in lateral flow assays. They are used for visual detection in 'presence or absence' testing. Fluorescent nanoparticles were used to obtain quantitative data from the test strips. It is hypothesized that the assay's limit of detection will decrease when using the fluorescent reporter. Both reporters have the same oligonucleotide sequence immobilized on the surface.

Gold nanoparticle functionalization

Streptavidin dressed gold nanoparticles (GNPs; BioAssay Works, Maryland) were used as the control reporter in the assay. The GNPs measured about 40nm in diameter. Before the reporter sequence could be added, the GNPs were diluted with water from OD_{520} of 15 to OD_{520} of 1. The biotin terminated reporter sequence was diluted with PBS to a final concentration of 24μM and added to the dilute GNPs. The GNP-DNA mixture was incubated at room temperature under 70 rpm rotation for 45 minutes. The GNPs were then blocked with 10% bovine serum albumin (BSA Fraction V; Fisher Scientific), filtered, pH 9.0 for 20 minutes under 20 rpm rotation at room temperature. The reporter was washed and concentrated by centrifuging at 3000-4000 x g for 20 minutes. The completed GNP reporter was held at OD_{520} of 1 in 2mM sodium borate buffer.

Fluorescent nanoparticle preparation and modification

Fluorescent nanoparticles were synthesized to be used in the assay to gain more quantitative data. Different surface modifications were explored to link the reporter sequence. After the assay was completed, the strips were analyzed with a plate reader and a dose response curve was constructed.

Fluorescent nanoparticle synthesis

Ruthenium ($Ru(bpy)_3^{2+}$) doped silica nanoparticle (SiNPs) were synthesized using a water in oil (W/O) emulsion according to the literature (Chang *et al*, 2006). Briefly, 1.77 ml triton X-100 (EMD, Germany), 7.5 ml cyclohexane (Fisher Scientific, Pittsburg, PA), 1.8 ml hexanol (Acros Organics, New Jersey), and 0.34 ml of 0.04 mol/L ruthenium (Sigma Aldrich) were combined in a beaker and stirred with a magnetic stir bar for 30 minutes at 600 rpm. One hundred microliters of tetraethyl orthosilicate (TEOS; Sigma Aldrich) and 200 μL ammonia (Acros Organics, New Jersey) were then added. The mixture was left to react for 24 hours under stirring at 600 rpm. The reaction vessel was covered in foil to prevent photobleaching of the ruthenium. Synthesis was carried out in a fume hood to prevent the escape of ammonia and other chemical vapors.

The nanoparticles were washed and concentrated after formation. The emulsion containing the SiNPs was transferred to a round bottom oak ridge centrifuge tube (Fisher Scientific) and 20 ml of acetone (Fisher Scientific) was added. The mixture was sonicated for five minutes in a sonicating bath then centrifuged at 4°C at 12000 rpm for 10 minutes. The supernatant was discarded and the particles were washed three times with ethanol (Fisher Scientific) and three times with water using the same procedure. The washed SiNPs were held in 5 ml of water until needed for surface modification.

Avidin Surface Modification

Modification involved coating the SiNPs with avidin, then cross-linking the avidin with glutaraldehyde to improve the stability of the protein on the surface (Zhao *et al*, 2010). To do this, one milliliter of the prepared SiNPs were centrifuged at 1.5xg for 15 minutes and the supernatant was discarded. One milliliter of 10mg/ml avidin solution

(Pierce, Rockford, IL) was added. The solution was incubated for 24 hours in 10 mM phosphate buffer (2.0078 g NaCl, 0.0505 g KCl, 0.3610 g Na_2HPO_4, 0.0608 g KH_2PO_4; pH 7.5) at 7°C on a vortex set to 600 rpm. Protein was also adsorbed to the nanoparticle surface at room temperature on a rotator set to 40 rpm. In the room temperature experiment, 150 μL of 5mg/ml avidin was added along with 3 ml of 10 mM phosphate buffer. After both experiments, the particles were washed three times with PBS by centrifuging at 1.5 x g for 15 minutes. A 1% glutaraldehyde (Alfa Aeser, Ward Hill, MA) solution was added and incubated for one hour under rotation (40 rpm) at room temperature. To make this solution, 40μL of 25% glutaraldehyde was added to 960μL PBS. After washing three times with PBS, unreacted aldehyde groups were blocked with 1 M Tris-HCl (pH 7.0). One milliliter of the Tris-HCl was added to the nanoparticles and incubated under rotation (40 rpm) at room temperature for three hours. The particles were washed three times in PBS as described above and held in 500μL of PBS until needed.

The amount of protein on the surface of the particles and from the supernatant taken from the first washing step was measured using the Bicinchoninic Acid (BCA) Protein Assay Kit from Thermo Scientific Pierce (Rockford, IL). The procedure was carried out in a 96-well plate and the absorbance was read at 562nm. A standard curve was constructed and used to determine the amount of protein on the surface of the particles and in the supernatant. Transmission electron microscopy was used to view the completed SiNPs to determine size distribution and shape.

Further modification involved linking the biotin-terminated reporter sequence to the avidin on the surface. Before hybridization, the nanoparticles were centrifuged as

above to remove the supernatant. Twenty microliters of 300μM biotin-terminated DNA was added to 480 μL PBS before being added to the SiNPs. The particles were left on a rotator set at 40 rpm for about 15 hours. Excess DNA was removed by centrifugation at 1.5 x g for 15 minutes. The modified SiNPs were held in 500μL PBS until needed.

Silane Surface Modification with APTMS

Silane groups were added to the surface of the SiNP to attach the reporter sequence (Chang *et al*, 2006). To begin, 500 μL of the SiNP were centrifuged at 10,000 rpm for 2 minutes in a benchtop centrifuge. The supernatant was discarded and 1 mL of 2% (v/v) (3-aminopropyl)trimethoxysilane (APTMS; Gelest, Inc, Morrisville, PA) in 95% ethanol was added. This was held at room temperature on a vortex at 600 rpm for 30 minutes. The particles were centrifuged at 10000 rpm for 2 minutes and the supernatant was discarded. They were washed once in ethanol and then in water by centrifuging at 10000 rpm for 2 minutes. After the supernatant was discarded and the new solvent was added, the centrifuge tube was placed briefly in a sonicating bath to resuspend the pellet. A 5% glutaraldehyde (Alfa Aeser, Ward Hill, MA) solution was added and incubated for 2 hours at 37°C on a vortex set to 600 rpm. After centrifuging to remove the glutaraldehyde solution, the SiNPs were washed once in PBS as described above. Ten microliters of amine-terminated reporter probe, 940 μL PBS and 50 μL 20X SSC (3.0 M NaCl, 0.3 M $Na_3C_6H_5O_7$) were added and mixed continuously for 2 hours at 37°C. The reporter probe had a concentration of 300 μM. After incubation, the particles were centrifuged to remove excess reporter probe and washed once in PBS as described above. The final step required the addition of 1 mL of 30mM glycine solution and

incubation at room temperature under shaking. The particles were washed and held in PBS until needed.

Silane Surface Modification with GPTMS

A third method of fluorescent nanoparticle modification was also tested (Zhang *et al*, 2009). Silane groups were deposited on the surface through the addition of (3-glycidoxypropyl)trimethyoxysilane (GPTMS; Acros Organics) and amine-terminated DNA was then linked to the surface. After synthesis, the nanoparticles were dialyzed in water for 48 hours to remove free dye and other contaminants from the water phase. The particles were then washed twice in ethanol by centrifuging at 12,000 x g at 4°C for 30 minutes. The treated particles were allowed to dry in a vacuum oven overnight at 25°C and 25" Hg. The weight of the dry nanoparticles was obtained and approximately 2 mg was used for further modification.

The reserved portion of dried nanoparticles was re-suspended in 4.5 ml toluene in a glass vial and sonicated in a bath for 1 hour. Five hundred microliters of 10% (v/v) GPTMS was added and the vial was transferred to a 65°C water bath to incubate for 2 hours under shaking at 200 rpm. The solution was transferred to five Eppendorf tubes before being centrifuged at 10,000 x g at 4°C for 30 minutes. The supernatant was discarded. The particles were then thoroughly washed. Six hundred microliters of toluene was used to centrifuge at 6,000 x g at room temperature for 2 minutes. The supernatant was discarded and replaced with 0.6 ml acetone. The particles were centrifuged at 7,000 x g at room temperature for 2 minutes, the supernatant was discarded, and they were washed again in acetone. The particles were washed twice in ethanol by centrifuging at 6,000 x g at room temperature for 2 minutes. The solution was

transferred to new tubes before the second wash. After washing, the particles were left to dry overnight in a vacuum oven set to 25°C and 25" Hg.

Amine-terminated reporter sequence (Table 3.1) was then conjugated to the modified nanoparticles. PBS (pH 6.8) was used to re-constitute the dry nanoparticles. The particles and DNA were transferred to a 10ml glass vial and put in a 37°C water bath under shaking at 200 rpm to incubate for approximately 48 hours. The final steps include centrifuging at 3500 x g at room temperature for 2 minutes to collect the completed particles and then washing in 0.6 ml PBS by centrifuging at 3500 x g at room temperature for 2 minutes. The nanoparticles were held in 100µl PBS until needed.

Assay conditions

The assay was performed in dipstick format in 10 ml glass culture tubes (Fisher Scientific). The target sequence was diluted to concentrations of 50-0.25 fmol/µL with PBS. The PBS was used as a control (0 fmol/µL). The reporters were further diluted before use. Five microliters of reporter (GNP or SiNP) and 2µL target (positive or negative control) were added to the culture tubes. PBS was added to bring the volume to 10 µL. The reporter and conjugate were allowed to incubate on the bench top for five minutes before the lateral flow strip was added. During the incubation period, the small bit of plastic at the end of the lateral flow strip was removed. The lateral flow strip was added to the tube with the absorbent pad on top. After one or two minutes, the strips were moved to a second set of tubes containing 35 µL of PBS, which acted as a running buffer to drive the reporter towards the reaction zone and reduce background. After ten minutes, the strips were removed and allowed to air dry briefly before analysis.

When using the GNP, visual inspection was sufficient to determine the outcome of the test. Two red lines indicated a positive test and one red line indicated a negative test. The SiNPs were not visible, so the strips were loaded into a modified 96-well plate to be read in a Biotek plate reader. This modified plate is shown in Figure 3.1. Shallow wells corresponding to the rows of a regular 96-well plate held the lateral flow strips in place (Figure 3.1A). A lid was placed on top that had holes exposing the areas of columns 4, 6, 7, and 8 or the beginning of the strip, the test line area, the control line area, and the absorbent pad, respectively (Figure 3.1B). The plate was read at an excitation wavelength of 460 nm and emission wavelength of 620 nm.

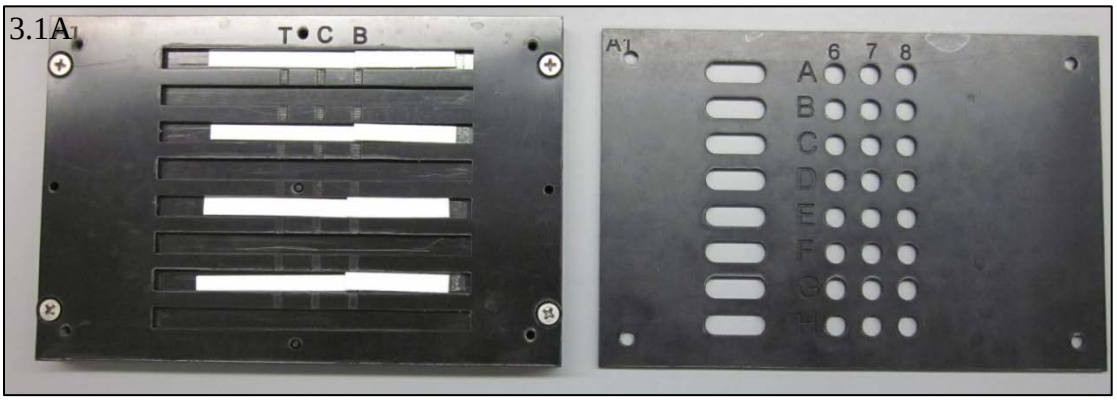

Figure 3.1A- The modified 96-well plate used to analyze the fluorescence produced by the ruthenium-doped SiNPs. The bottom of the plate is shown on the left. Shallow trenches hold the test strips in place. Small grooves were cut to line up the test line (T) and control line (C) with openings in the lid. The lid is shown on the right. The oval holes expose the bottom of the test strip, the holes in columns 6, 7, and 8 expose the test line, control line, and absorbent pad, respectively.

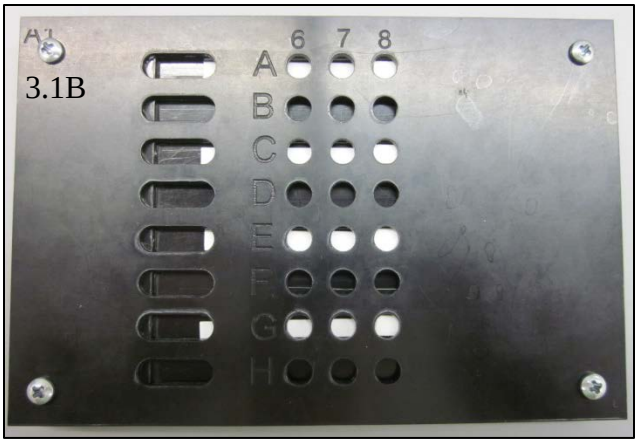

Figure 3.1B- The assembled 96-well plate used to measure fluorescence produced by the ruthenium-doped SiNPs. The lid was placed on top of the tray holding the test strips and was held in place with screws. The exposed areas were read by the Biotek plate reader much like a normal 96-well plate.

Results

Effects of blocking

The nitrocellulose reaction chamber must be blocked with proteins to prevent the streptavidin coated gold nanoparticles (GNPs) or avidin coated ruthenium doped silica nanoparticles (SiNPs) from adsorbing to the membrane. Experiments were performed to determine the optimal blocking dilution and time for the membrane. The composition of the blocking buffer was described previously. The membranes were blocked in stock concentration of buffer and varying concentrations that involved diluting the buffer with water. Plain water was used to act as a control. These dilutions are given in Table 3.2. The results of blocking time are not shown, but blocking time ranged from 1 to 30 minutes.

Table 3.2. List of the concentrations of blocking buffer used to treat the nitrocellulose membrane.

LF Strip ID	X parts blocking buffer : Y parts water
A (stock concentration)	1:0 (all blocking buffer)
B	1:1
C	1:2
D	1:3
E	1:4
F	1:5
G (control)	0:1 (all water)

The results of varying buffer dilution are shown in Figure 3.2. The labels A through G correspond with the details in Table 2. In Figure 3.2, strip G was blocked with water (control). The pink patch on the right shows the place where the GNPs were added to the strip. They were unable to flow up the strip. Strips C through F show limited movement of the GNPs up the strip due to the pink smears on the right side. These strips were blocked with one part blocking buffer and increasing parts water.

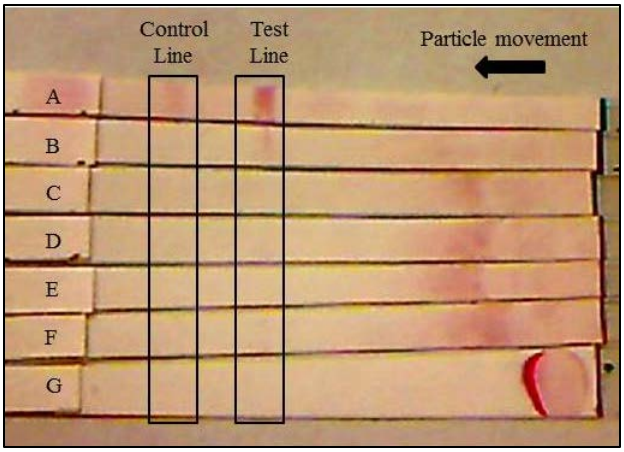

Figure 3.2- Effects of blocking on GNP reporter movement up the nitrocellulose membrane. Strip A shows optimal movement because the test and control lines are visible, while Strip B shows only an incomplete test line. Strips C-F show impaired reporter movement due to lack of blocking. Strip G was treated with water and shows limited movement of the reporter because the avidin is adsorbing to the nitrocellulose membrane.

In Figure 3.2, strip B shows better movement of the GNPs than strips G through C because a partial test line is formed. Strip A shows optimal movement up the strip

because the GNPs were able to reach the reaction zone. A strong test line and weak control line are visible on the test strips treated with stock blocking buffer. The test strips were then treated for varying times to determine optimal blocking time. It was discovered that treating the test strips for 1 minute with stock concentration of blocking buffer provided the appropriate amount of coverage to allow the GNPs to reach the reaction zone of the test strip.

GNP reporter optimization

Optimal GNP reporter concentration was also determined. The particles needed to be dilute enough to flow through the NC without aggregation, yet concentrated enough to provide a strong signal. It was found that using a concentration of OD_{520} 2.3 worked best. Higher concentrations were used, but the GNPs became trapped in the test line and produced an invalid result because the control line did not develop. Lower concentrations produced weak signals.

GNP reporter results

Assays were performed to validate the construction of the lateral flow cards and then to test their working range. Synthetic target, which mimicked a portion of rRNA found in Eukaryotic organisms, was diluted to a range of 50 to 0.25 fmol/μL. PBS was used as a negative control (0 fmol/μL). The tests were performed in dipstick format in glass culture tubes. Results from triplicate tests are shown in Table 3.3. The results show that 10 fmol of target was consistently detected using the assay, although the first test detected 5 fmol. Figure 3.3 shows typical results from the test. The appearance of a control line indicated a valid test run.

Table 3.3. Results from triplicate testing using GNP as reporter.

Total target concentration (fmol/2 µL)	Test 1	Test 2	Test 3
0	-	-	-
0.5	-	-	-
1	-	-	-
5	+	-	-
10	+	+	+
25	+ +	+ +	+ +
50	+ + +	+ + +	+ + +
100	+ + +	+ + +	+ + +

Ten femtomoles of target was consistently detected using this reporter. The first test was able to detect 5 fmol, but the next two tests were unable to do this. One plus sign (+) represents a weak test line signal, two plus signs (+ +) represent a slightly stronger test line signal, and three plus signs (+ + +) represent a very strong test line. All control lines appeared strongly (+ + +). Each test was valid due to the appearance of a control line.

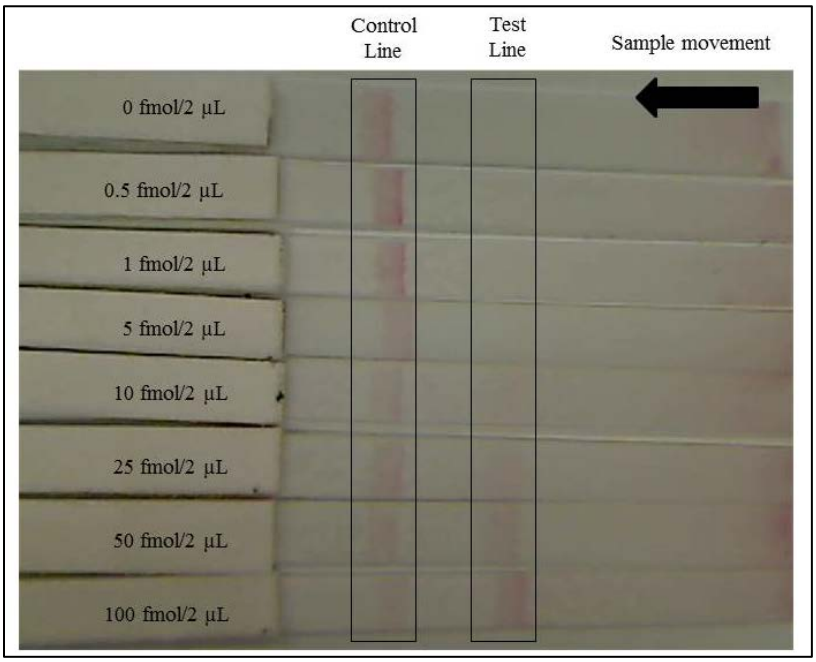

Figure 3.3- Typical results of the assay using GNP as reporter. The target concentration is listed on the left and the direction of sample movement is indicated. Each test is valid due to the development of a control line. Higher sample concentrations lead to darker test lines. This format is best used for presence/absence testing.

The average grey value of the test lines was also analyzed using Adobe® Photoshop® CS5.1 Extended to obtain more quantitative data. The results are shown in

Table 3.4. Grey scale values range from 0-255, with 0 representing pure black and 255 representing pure white. The test lines from the higher concentrations showed a darker, more intense red color and therefore received a lower value, while the test lines from the lower concentrations had less red color and received a higher value. This relationship is also shown graphically in Figure 3.4.

Table 3.4. Mean Grey Value of test lines from GNP assays.

	Mean Grey Value			
Total Target Concentration (fmol/2 µL)	Trial 1	Trial 2	Trial 3	Average Grey Value
0	102.72	119.00	121.27	114.33
0.5	106.38	121.66	126.29	118.11
1	111.69	132.05	131.81	125.18
5	108.47	132.37	129.58	123.47
10	101.97	121.53	122.82	115.44
25	95.84	116.13	117.27	109.75
50	87.98	104.96	102.44	98.46
100	79.95	94.12	88.42	87.50

The grey value of the test line was measured in Photoshop. Lower values correspond to darker, richer colors while higher values correspond to brighter, whiter colors. After the first two points, grey value is inversely proportional to target concentration.

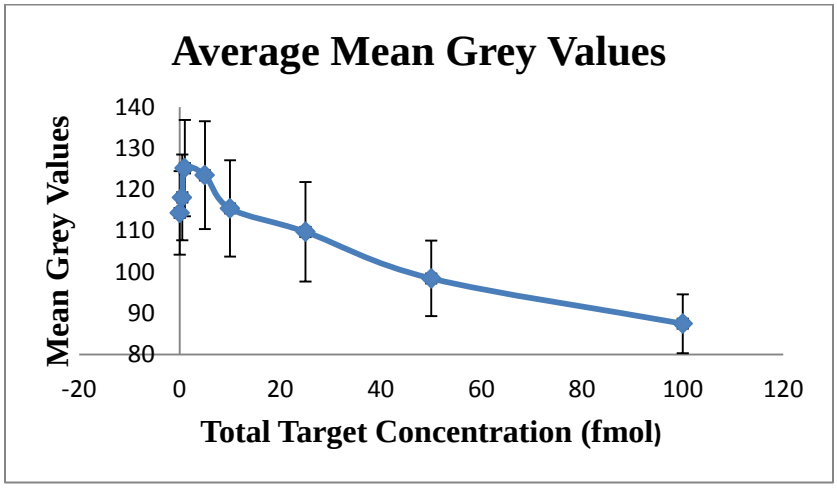

Figure 3.4- Graph of the Mean Grey Values for the test line in the assay using GNP as reporter. Using this graph along with Figure 3.3, it is easy to see that the highest target concentration has the lowest mean grey value and the strongest test line signal. Test line intensity decreases with decreasing target concentration.

$Ru(bpy)_3^{2+}$ doped silica nanoparticle synthesis and use

Ruthenium doped silica nanoparticles (SiNPs) were synthesized using a modified Stöber method, which involves forming a water in oil (W/O) emulsion. Surface modification involved coating with avidin to allow the linking of biotin-terminated reporter DNA, much like the GNPs. Experiments were also conducted to deposit silane groups on the surface and link amine-terminated reporter probe.

Transmission electron microscopy (TEM) was used to image the SiNPs. Figure 3.5 shows a sample of SiNPs modified with avidin. Carbon coated copper grids were used for the TEM. The SiNPs were first sonicated in ethanol for three minutes then applied to the copper grids. After the grids were dried, they were viewed. The particles are round, uniform in size, and concentrated. They are approximately 70 nm in size. Although this is larger than the 40 nm GNP reporter, proper dilution of the SiNPs and treatment of the surface allowed movement up the NC test strip.

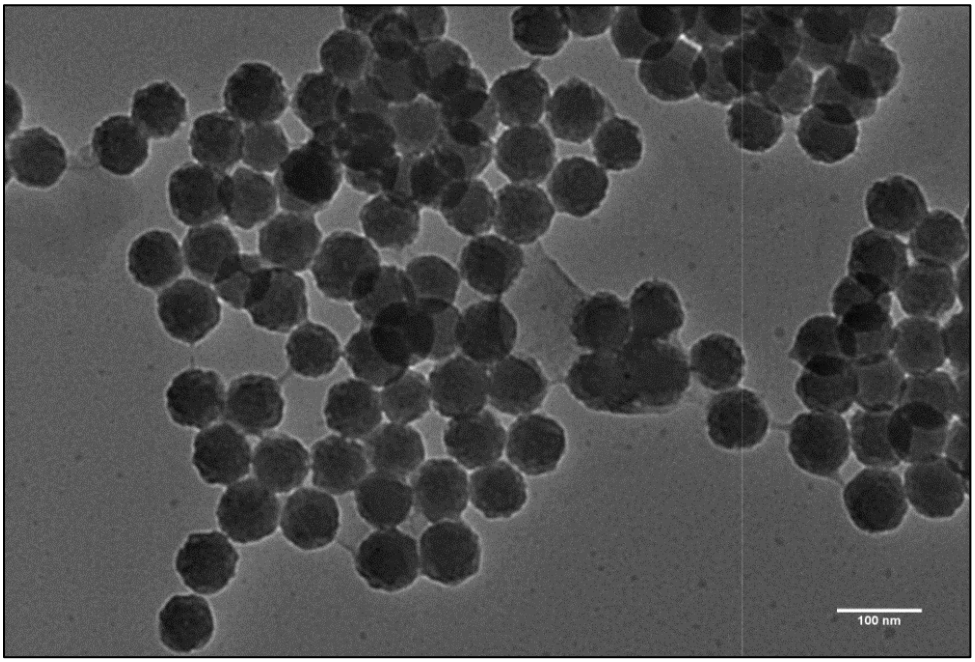

Figure 3.5- Ruthenium-doped SiNPs synthesized by W/O emulsion. The ruthenium core is darker than the surrounding silica shell. The particles are approximately 70 nm in diameter and are uniform in size and shape.

In order to determine the amount of biotin-terminated reporter probe to add to the SiNPs, the amount of surface avidin must be determined. This was accomplished using the BCA assay. Figure 3.6 shows the standard curve generated from this assay. Initially, 150 µL of 5 mg/ml solution of avidin was added to the SiNPs which were then incubated at room temperature on vertical rotator. The BCA assay showed the stock concentration of SiNPs had approximately 368.55 µg of avidin per milliliter of nanoparticle. This corresponded to an approximate concentration of 5.6 nmol (10^{-9}) avidin. Avidin is a tetrameric protein capable of binding four biotin molecules. This amount of avidin was able to bind about 22.4 nmol of biotin.

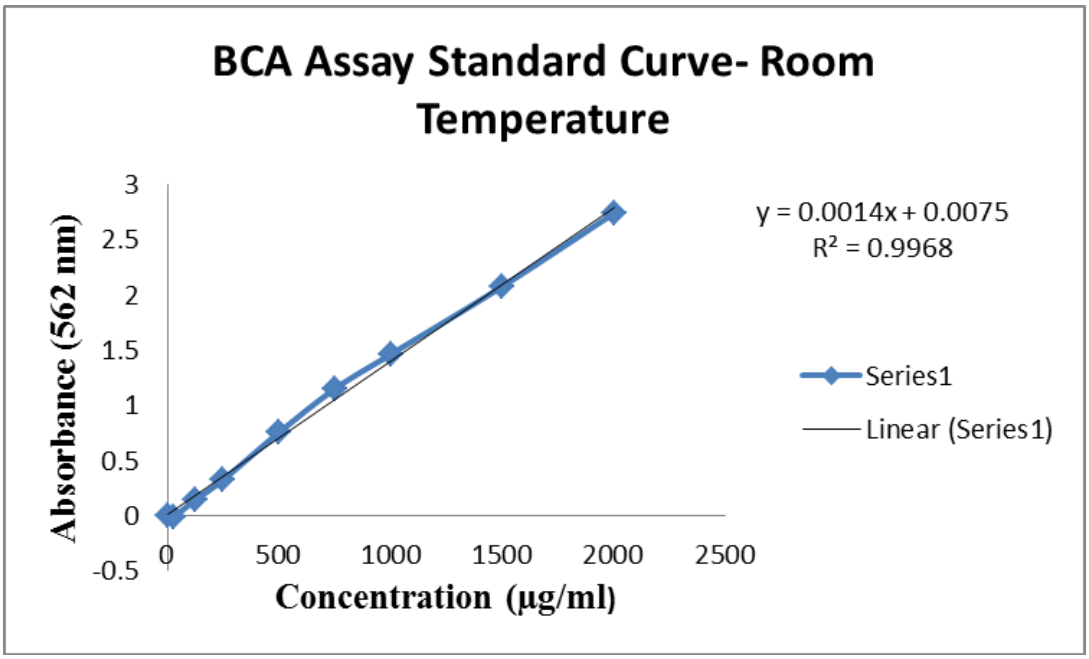

Figure 3.6- Standard curve generated from the BCA assay used to determine protein content on SiNP surface when adsorbed at room temperature.

However, this was not enough avidin to bind the appropriate amount of reporter probe to the surface. One hundred microliters of 300 µM biotin-terminated reporter probe was added to the SiNPs. This is equivalent to about 30 nmol of biotin-terminated probe. There was not enough reporter probe immobilized on the SiNP to bind to the test

and control lines in the reaction zone. Results are shown in Table 3.5. The SiNPs were diluted to OD_{620} of 1 before use. Absorbent pads CF3, 4, and 5 were used. The pads differ in the amount of liquid they can hold and wicking rate, with 3 being slowest and 5 being fastest. PBS was used as a negative control and a total of 100 fmol of target sequence was used as a positive control. The protocol describes previously was followed for testing the samples. The test strips were analyzed with the Biotek plate reader at an excitation wavelength of 460 nm and emission wavelength of 620 nm.

Table 3.5. Fluorescence data in arbitrary units (AU) from lateral-flow strips using OD_{620} 1.0 SiNP as reporter.

Test Strip ID	Bottom of Test Strip	Test Line	Control Line	Absorbent Pad
CF3 (-)	3388	342	335	1248
CF3 (+)	4147	357	342	929
CF4 (-)	2818	379	325	1810
CF4 (+)	3724	349	341	1436
CF5 (-)	2376	692	752	3482
CF5 (+)	4320	397	408	2736

This shows the SiNPs and target sequence did not hybridize to the reaction zone. The fluorescence readings for the test and control line are approximately the same and have rather low readings. The SiNPs were trapped in the bottom of the test strip. A portion of the SiNPs was able to travel up the test strip to the absorbent pad. These results could be due to inadequate avidin adsorption to the nanoparticle surface. If the surface is not fully coated, the biotin would not have a place to bind and the nanoparticle would not have enough reporter probe to be able to hybridize to the reaction zone.

The experiment was repeated using a higher concentration of avidin and adsorbing the protein to the surface at 7°C using a vortex mixer. One milliliter of 10mg/ml avidin was added to the SiNPs. The BCA assay was repeated and used to

measure the protein on the SiNPs and in the supernatant from the first washing step after adsorption. Figure 3.7 shows the standard curve constructed from this assay. The stock concentration of nanoparticles had approximately 156.33 µg/ml of avidin adsorbed on the surface. This is equivalent to 2.37 nmol of avidin. It would be able to bind 9.48 nmol of biotin. The supernatant from the first washing step contained 7776.67 µg/ml of avidin. Twenty microliters of 300 µM reporter probe was added. The reporter was used in an assay and the results were analyzed.

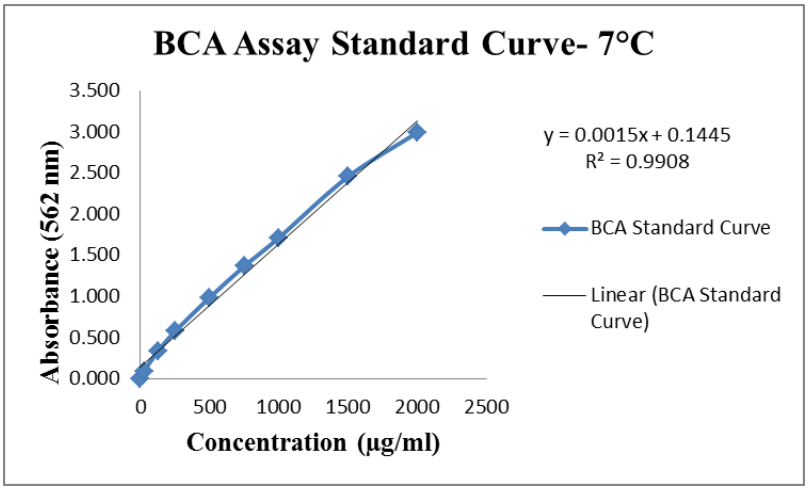

Figure 3.7- Standard curve generated from the BCA assay used to determine protein content on SiNP surface and supernatant when adsorbed at 7°C.

The optimal concentration of nanoparticles was obtained by diluting the SiNPs by 100. This allowed all of the nanoparticles to travel up the nitrocellulose reaction chamber without clogging the pores. This dilution factor was used when comparing three types of modified SiNPs- avidin modified, APTMS modified, and un-modified SiNPs. Each test strip used CF5 absorbent pad. Again PBS was used as a negative control and 100 fmol of target sequence was the positive control. The results are shown in Table 3.6.

Table3.6. Comparison of three ruthenium-doped SiNPs used as reporter.

Reporter ID	Bottom test strip	Test Line	Control Line	Absorbent pad
Avidin (+)	357	642	607	3209
Avidin (-)	291	598	542	2873
Silane (+)	468	585	497	3252
Silane (-)	648	591	529	3478
Un-mod (+)	488	500	458	4072
Un-mod (-)	387	600	585	3322

The avidin was adsorbed to the surface through Zhao's method, the silanes were deposited by APTMS through Chang's method, and 'un-mod' particles do not have any surface modification.

The SiNPs were all diluted 1:100 before use. Experiments were performed with various other dilutions, but most of the nanoparticles remained clogged at the beginning of the test strip (data not shown). Again, neither surface modification was able to hybridize in the reaction zone. The fluorescence readings from SiNPs that had reporter probe added were the same as fluorescence readings from SiNPs that did not have reporter probe added. The high readings from the absorbent pad are from the collected SiNPs.

The SiNPs modified with GPTMS were also tested. The reporter was used as collected. A kinetic read was used to analyze the strips in the Biotek. One reading was taken every minute for 70 minutes. The sum of the test line measurements was used. Concentrations from 0-12.5 fmol were tested. The graph of the GPTMS reporter is shown in Figure 3.8. GPTMS modified fluorescent SiNPs were able to detect 0.027 fmol of target sequence.

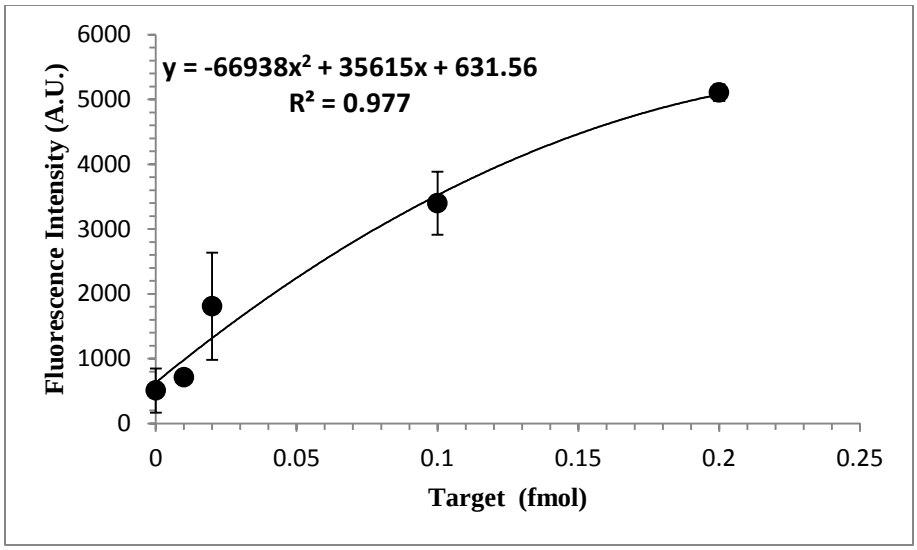

Figure 3.8- Graph of GPTMS modified SiNP reporter. Error bars with standard deviation are shown. This method was able to detect 0.027 fmol of target sequence.

Discussion

Rapid testing methods are becoming increasingly popular in many sectors. Lateral-flow test strips are transportable, easy to use, and require minimal sample preparation. Commercial products are contained in plastic cassettes that protect the inner components and allow for easy handling. The novel test was used in dipstick format; the nitrocellulose of the test strip was added directly to the reporter conjugate and purified sample. Commercial products use a sample pad to filter out undesired or inhibitory elements in the sample and a conjugate pad that contains dried reporter conjugate. These parts were not used in the novel test method because proof of principle was being shown. Figure 3.9 shows a novel test strip in a commercial plastic cassette. It is small and compact. The sample would be applied through the small opening on the left and the test and control lines are visible through the labeled viewing window. In a clinical setting, sample identification can be written on the cassette to avoid confusion. A desiccant pack

can be stored next to the test strip to reduce the humidity inside and prolong the shelf life of the assay.

Figure 3.9- Novel test strip housed in a commercial plastic cassette.

Proper assembly of the lateral flow test strip is essential for a valid assay. Blocking the nitrocellulose membrane is necessary to enable uninhibited reporter and target movement towards the reaction zone. Streptavidin and other proteins adsorb easily to nitrocellulose. This is seen in strip G of Figure 3.2. A large portion of GNPs were added to the bottom of the test strip and were unable to move past their entry point. At least 100 μL of PBS was added to the strip to wash the nanoparticles up the strip but they didn't move. The nitrocellulose was treated with a casein solution to deposit proteins throughout the porous membrane. Casein and the other components of the blocking buffer did not interact with the GNPs and helped them move up the test strip.

Using the appropriate amount of reporter in the assay is also important. If the reporter is too concentrated, the membrane will be saturated with nanoparticles and movement will be hindered. This was observed with both gold and fluorescent nanoparticles. When concentrated GNPs were used, they were stuck behind the test line and could not reach the control line. This imitated an invalid test because the control line

did not appear. The correct dilution of GNP was found by running a series of dilutions until both test and control lines appeared. When using the fluorescent nanoparticles, they were stuck at the bottom of the test strip. Each particle was about 40 nm wider in diameter than the gold nanoparticles. When concentrated, they were unable to travel towards the reaction zone. The fluorescence detected in the absorbent pad could be free ruthenium or smaller nanoparticles that were able to travel up the strip. After the correct concentration was determined, fluorescence was no longer detected at the bottom of the test strip.

Using GNP as a reporter works best for visual determination of a positive or negative result. The test and control lines are red in color, easy to see with the naked eye, and permanent so analysis can be performed when it is convenient for the technician. The test is also easy to interpret and dispose of. GNP reporter is best used for presence or absence testing because it is difficult to correlate test line intensity with target concentration. Software was used to measure the grey value of the test line. Grey value is used to measure brightness and ranges from 0 to 255. Zero intensity is black and full intensity is white. Darker and more intense colors have lower grey values while lighter and less saturated colors have higher grey values. The color intensity of the test lines decreased as the target concentration decreased until the target concentration was below the test's limit of detection. It was observed that 100 fmol sample had the darkest test line and lowest average grey value. Figure 3.4 shows a small decrease in grey value for 0 and 0.5 fmol but that is due to uneven exposure of the image. The edges of the picture were darker and lead to false values. If the photograph was evenly exposed, the graph would be more linear and the error bars would be smaller.

Fluorescent silica nanoparticles (SiNP) were used to obtain more quantitative data. Ruthenium was chosen because it is water soluble, safe to use and easy to dispose of. Using the modified Stöber method produced nanoparticles that were concentrated and uniform in size and shape. The particles were approximately 70 nm in diameter. The size is depended on reaction time and the amount of reagents used. In Figure 3.5, the ruthenium is visible in the core of the nanoparticle because it is more electron dense than the silica that surrounds it. In a transmission electron microscope, or TEM, a beam of electrons is passed through a sample and focused through several lenses before being magnified on a viewing screen. It is a valuable tool in viewing objects that are too small to be viewed with a light microscope.

The surface of the SiNP was modified several ways to immobilize the reporter sequence to the reporter. Avidin coating was attempted first because the GNPs were streptavidin dressed. Differing avidin concentrations and adsorption temperatures were investigated and the amount of avidin was measured with the BCA assay. It was observed that using a rotator that turned the SiNPs end over end was able to deposit more avidin on the NP surface than a vortex mixer that rapidly shook the SiNP. The SiNPs on the rotator had three times more avidin on the surface than the SiNPs on the vortex mixer. Temperature was also investigated but it didn't seem to have as big of an effect as the type of agitation.

The BCA assay is a colorimetric method used to detect and quantify total protein. It combines the reduction of Cu^{2+} to Cu^{1+} by protein in an alkaline medium with the selective and sensitive colorimetric detection of the cuprous cation (Cu^{1+}) using bicinchoninic acid (Smith *et al*, 1985). A purple color develops when two molecules of

BCA are chelated with one cuprous ion. The complex absorbs at 562 nm and has a working range of 20-20,000 μg/ml. A standard curve is generated and then used to determine the protein concentration of the unknown sample. The BCA assay was an easy and accurate way to measure the amount of avidin adsorbed on the SiNP surface.

The amount of avidin was used to calculate the amount of biotin that can be bound. An excess of biotin-terminated reporter probe was added to the SiNP. However, the avidin coated SiNPs did not bind to the reaction zone. The fluorescence detected by the reaction zone was similar to that detected at the bottom of the test strip. There are several reasons why this could have happened. The avidin may have fallen off the surface or was damaged during the washing steps and therefore the reporter probe was unable to bind to the surface. The protein may not have fully coated the surface due to lack of electrostatic attraction. This could have been due to the buffer the SiNPs were held in. If the buffer was completely dialyzed away from the particles, the surface charge would have changed and the protein may have been more attracted to the surface. Without sufficient reporter probe attached to the nanoparticle, it would not be able to hybridize in the reaction zone. The capillary forces would pull the SiNP away from the reaction zone, resulting in invalid results.

The GPTMS modified SiNPs were successfully used as a reporter in the assay. The APTMS may not have adsorbed to the surface properly because of the salts from the buffer that the particles were held in. The GPTMS particles were dialyzed in water overnight to remove all buffer salts and impurities in the water phase. Reaction temperature may have affected the outcome of the modifications. The APTMS modifications were carried out in a vortex mixer in a walk-in incubator that was heated

by air and the GPTMS modifications were carried out in a heated shaking water bath. Water has better heat transfer than air and the agitation from the water bath kept the particles suspended in the reaction solution better than the vortex mixer.

A kinetic measurement was used because the larger SiNPs may have been delayed in traveling through the pores of the NC membrane. Although a kinetic measurement was not used for the avidin or APTMS modified SiNPs, the strips were analyzed at intervals of 10 minutes to determine if a test or control line developed.

As hypothesized, the novel method was more sensitive than the standard method. This could be to the result of a more sensitive detection method. GNP reporters could have hybridized to the test line at concentrations below 10 fmol, but the eye could not detect it. Using the Biotek plate reader may have shown a lower limit of detection. A 'hook effect' is seen with the GPTMS SiNP (Koets *et al*, 2006). An assay can best detect target in the linear portion of the dose-response curve. As the target concentration increases past the working range, the assays sensitivity begins to decrease because the target is beginning to saturate the reporter conjugate and test line. The reporter cannot bind to the test line due to steric hindrance and the signal decreases.

Conclusions

As the population increases and the demand for minimally processed foods increased, rapid testing methods will become indispensable. A novel lateral-flow test was developed to detect yeast oligonucleotide sequences. Gold nanoparticles were used as a standard reporter and were compared to a novel fluorescent nanoparticle. Streptavidin dressed GNP were linked to the reporter sequence with biotin. The standard method was able to detect 10 fmol of target. Ruthenium-doped silica nanoparticles were

synthesized with a modified Stöber method. The particles modified with avidin and APTMS were unable to detect target sequences because the particle surface was unsuccessfully modified and sufficient reporter probe could not be immobilized. However, modifying the surface with GPTMS successfully detected 0.027 fmol of target sequence. The improved limit of detection is due to a more sophisticated detection method. To further improve the assay, the SiNP concentration and amount of reporter sequence on the surface could be optimized.

CHAPTER 4

ADDITIONAL WORK

Review of food borne biological warfare

Brief introduction to food borne biological warfare

Throughout history, bioterrorism and biological agents have been widely used. From the use of Plague infected corpses and Smallpox-contaminated blankets in centuries past, to *Bacillus anthracis* spores being sent through the mail in Fall 2001, the threat of a bioterrorist attack has been ever present. There are several political, social, economic, and religious reasons for these attacks. During World War II, Churchill knew of German rockets containing biological agents and prepared to retaliate by dropping anthrax-laced cattle cakes on the German countryside to ruin the beef supply (Bhalla, 2004). Chilean grapes were found to contain small amounts of cyanide in the late 1980s (Grigg and Modeland, 1989). Although fatalities were not encountered, Chile's reputation and economy were disrupted. A religious cult in Oregon contaminated several salad bars with *Salmonella typhimurium* type 2 in the 1980s. Their plan was to make voters sick and influence outcome of an election on land use (Török *et al*, 1997). On a smaller scale, a hospital worker in Texas was suspected of contaminating food in the staff break room with *Shigella dysenteriae* stolen from the hospital's lab (Kolavic *et al*, 1997). If a national chain such as Kraft or Campbell's was infiltrated and contaminated, the effects on the population would be devastating.

Yersinia pestis, *B. anthracis*, and *Salmonella typhi* are considered 'classic' agents of biological warfare. They are related to food borne pathogens and have similar virulent

factors. Food suppliers can be contaminated with *Yersinia enterocolitica*, *Bacillus cereus*, and Salmonella species and affect millions of people. Typical food borne pathogens such as *Escherichia coli* O157:H7, *Vibrio cholera*, and *Coxiella burnetti* have been used in bioterrorism. *Clostridium botulinum* and *Staphylococcus aureus* produce toxins that are a problem in the food industry and can be intentionally used to harm a population. Viruses such as Norovirus and Variola major, the cause of Smallpox, can be added to food and infect a large portion of the population.

The federal government and similar agencies test for these contaminants using immunological technology and nucleic acid-based techniques that are rapid, easily interpreted, and highly accurate. The food industry comes into contact with many of the same contaminants, but relies on traditional microbiological test that are time consuming and sometimes misinterpreted. Why is the food industry slow to adopt new detection methods?

Biological agents- definitions and CDC classification

According to the Department of Homeland Security, a biological agent (BA) is any "toxin, bacterial, or viral organism that can cause casualties when released. To be an agent, it must be infectious to humans, capable of being produced in enough quantity to be toxic and stable through the dissemination process" (Fatah *et al*, 2007). Biological agents are also characterized by low visibility, high potency, accessibility, and ease of transportation and dissemination (Danzig and Berkowsky, 1997). The Centers for Disease Control and Prevention (CDC) has organized biological agents into several categories based on their mortality rate, transmissibility, degree of public health preparedness, risk to national security, and several other criteria. Category A contains

top priority BAs that are easily passed from person to person, result in high mortality rates, and have the potential to cause a massive public health impact. These BAs might also cause public panic and social disruption and require special action for public health officials. The disease and causative agents found in Category A are listed in Table 4.1. Category B includes second priority BAs that are moderately easy to disseminate, result in moderate morbidity and low mortality, and require specific CDC diagnosis and enhanced disease surveillance. The disease and causative agents found in Category B are listed in Table 4.2. Category C contains the third highest priority agents that are emerging pathogens that have the potential to be engineered for mass dispersal because of availability, ease of production and dissemination, and a potential for high morbidity and mortality. Agents found in Category C are listed in Table 4.3 (Fatah *et al*, 2007).

Table 4.1. Category A diseases and causative agents

Category A diseases and causative agents (Source: Fatah *et al*, 2007)
• Anthrax (*Bacillus anthracis*) • Botulism (*Clostridium botulinum* toxin) • Plague (*Yersinia pestis*) • Smallpox (Variola major) • Tularemia (*Francisella tularensis*) • Viral hemorrhagic fevers (Filoviruses [ex Ebola, Marburg] and Arenaviruses [ex Lassa, Machupo]

Table 4.2. Category B diseases and causative agents

Category B diseases and causative agents (Source: Fatah *et al,* 2007)
• Brucellosis (*Brucella* species) • Epsilon toxin of *Clostridium perfringes* • Food safety threats (*Salmonella* species, *E. coli*, *Shigella*) • Glanders (*Burkholderia mallei*) • Melioidosis (*Burkholderia pseudomoallei*) • Psittacosis (*Chlamydia psittaci*) • Q fever (*Coxiella burnetii*) • Ricin toxin from castor beans • Staphylococcal enterotoxin B • Typhus fever (*Rickettsia prowazekii*) • Viral encephalitis (Alphaviruses ex Venezuelan equine encephalitis) • Water safety threats (Vibrio cholera, Cryptosporidium parvum)

Table 4.3. Category C diseases and causative agents

Category C diseases and causative agents (Source: Fatah *et al,* 2007)
• Emerging infectious disease threats such as Nipah virus, Hantavirus, Tickborne Hemorrhagic Fever viruses, Tickborne Encephalitis virus, Yellow Fever, and Multidrug-resistant Tuberculosis

Plague and Yersinia pestis

Yersinia species are gram-negative, oxidase-negative, facultative anaerobic bacteria that ferment glucose. There are 11 known species, four of which are pathogenic. *Y. pestis* causes the Plague, *Y. pseudotuberculosis* causes disease in rats and occasionally humans, *Y. ruckeri* causes disease in salmonoids and freshwater fish, and *Y. entercolitica* is the most prevalent *Yersinia* pathogen in humans. *Y. pestis* is dispersed through the bites of infected fleas or a respiratory aerosol, while *Y. pseudotuberculosis* and *Y. enterocolitica* are food borne pathogens. The food borne pathogens could theoretically be used as BAs, but they would not be as successful as *Y. pestis*. These four species have essential virulence factors. All are genetically similar, especially *Y. pestis* and *Y.*

pseudotuberculosis which share over 90% DNA homology. The species are hard to distinguish through traditional microbiological techniques and few novel ways have been developed.

Y. pestis and the Plague have been used in biowarfare since the Middle Ages. The causative bacterium is a naturally occurring pathogen and can therefore be prepared for use as a weapon by anyone with appropriate skills and facilities (Ertner *et al*, 2003). Once prepared, the pathogen could easily be spread through an aerosol. In 1970, the World Health Organization estimated that if 50 kg of *Y. pestis* was aerosolized over a city of 5 million, 150,000 would contract Plague and 36,000 of those infected would die (Inglesby *et al*, 2000). This is a frightening figure because a vaccine against the Plague is no longer available and the antibiotics used to treat the disease are in limited supply. *Y. pestis* would make a dangerous and effective biowarfare agent because of its availability, high mortality rate, ease of dissemination, rapid onset of symptoms, and limited treatment options (Ertner *et al*, 2003; Inglesby *et al*, 2000). Although Plague has never been successfully used for biowarfare, there have been instances where vials of bacteria have gone missing (Ertner *et al*, 2003).

Plague can present in two forms- bubonic and pneumonic. Bubonic plague is a primary infection spread by the bite of an infected flea. Pneumonic plague is spread through aerosolized droplets of bacteria. This can be done intentionally or intentionally by breathing on someone. Symptoms of bubonic plague, which include enlarge lymph nodes, septicemia, and gangrene, develop 1-3 days after infection and can last up to six days. If left untreated, fatality rates can range from 30-75%. Pneumonic plague occurs after the infection has spread to the lungs. Symptoms develop 1-6 days after initial

infection and include fever, chills, malaise, vomiting, coughing, bloody sputum, respiratory failure, and circulatory collapse. Pneumonic plague is highly contagious and results in death in 95% of cases, unless antibiotics are administered within the first 24 hours of symptom onset (Fatah *et al*, 2007; Ertner *et al*, 2003). It is easy to overlook the symptoms of pneumonic plague in the early stages of disease. Since antibiotics are not administered quickly and are in limited supply, the disease is almost always fatal.

The government and Homeland Security use several different types of detection methods to monitor *Y. pestis*. Many of these techniques analyze aerosolized bacteria or require extensive sample preparation. Meyer and colleagues (2007) have developed a biosensor to identify *Y. pestis* in different matrices. This novel method utilized magnetic beads and the bacteria's antigen fraction F1 to both detect and quantify the target in the sample. The biosensor has a detection limit of 2.5ng/ml in PBS buffer and a detection range of 25-300 ng/ml in human blood. This technique would be useful on the small scale.

Yersinia enterocolitica

Y. enterocolitica is a food borne pathogen that can survive in the intestinal tracts of mammals, birds, frogs, fish, flies, fleas, crabs, and oysters as well as water systems. It is frequently found in pork, beef, lamb, poultry, and dairy products. It has an infectious dose of 10^4 CFU and manifests as nonspecific, self-limiting diarrhea. These symptoms are mainly seen in children. In older children and teenagers, *Y. enterocolitica* infection is often mistaken for appendicitis.

This could be used for biological warfare because *Y. enterocolitica* readily withstands several freeze-thaw cycles, can survive in frozen foods, and can easily grow at

refrigeration temperatures in cooked foods. Cooked foods provide more available nutrients than raw food and the cooking process removes competitive bacteria. This pathogen has been isolated from pasteurized milk, pasteurized liquid eggs, vacuum-packed meat, cottage cheese, beef, pork, and seafood. Contaminated foods are re-inoculated after the cooking process because *Y. enterocolitica* and *Y. pseudotuberculosis* are killed by heat and pasteurization. However, it would not be an effective biological warfare agent because of a low morbidity and mortality rate, self-limiting infection, and mild symptoms. The organism is also easily destroyed through pasteurization.

As previously mentioned, *Yersinia* species can have up to 90% DNA homology. Distinguishing pathogenic from non-pathogenic species can be difficult. When grown on blood agar, *Yersinia* colonies are smaller than other Enterobacteriaceae colonies and can be overlooked. For this reason, Whittaker (2009) has developed a way to distinguish *Y. pestis* from other closely related *Yersinia* species. He used capillary gas chromatography with flame ionization detection (GC-FID) to determine the cellular fatty acid composition of six *Y. pestis* strains and then compared them to the compositions of other pathogenic and non-pathogenic *Yersinia* species. Analysis of the fatty acid profiles showed differentiation of the species. The method was sensitive, analytical, and useful of the small scale.

Anthrax and Bacillus anthracis

The *Bacillus cereus* group of bacteria are Gram-positive, rod shaped, aerobic spore-formers and include *B. anthracis*, *B. mycoicles*, *B. thuringiensis*, *B. pseudomycoides*, and *B. weihenstephanensis* (Granum, 2005). *B. cereus* is most common and is known to cause food poisoing, *B. anthracis* is most well-known for causing

Anthrax, and the other bacteria in the group have been used as pesticides. All species share a common ancestor and therefore have highly similar 16S and 23S rRNA sequences. Differentiating *B. anthracis* from other *B. cereus* bacteria in the early stages of infection is imperative to survival, but can be difficult because of the genetic homology. Novel ways have been developed to overcome this.

Bacillus anthracis is distinguishable from other members of the group by the presence of two virulence plasmids, pXO1 and pXO2 (Koehler, 2009; Khan, 2009). These plasmids contain the genetic information for anthrax toxin proteins and capsule proteins.

The bacterium requires a host for survival. Outside of a nutrient-rich environment, *B. anthracis* will sporulate into hardy spores that can survive for decades in harsh environment (Hang *et al*, 2008). *B. anthracis* spores are typically found in soil. Anthrax infection begins when the host comes into contact with the spores in the environment or an infected animal who obtained the spores from the environment. Person to person transmission of Anthrax has never been reported. Once ingested, the spores rapidly germinate, multiply, and cause infection. Anthrax will manifest in three forms- cutaneous, gastrointestinal and inhalation.

Cutaneous anthrax is the most commonly encountered form of the disease. Legions appear on exposed skin and eventually turn into large ulcers with black centers after coming into contact with an infected animal (Brook, 2002). The legions themselves are not fatal, but subsequent infections often lead to death. Without treatment, the fatality rate of cutaneous anthrax is 20%. The use of antibiotics reduces the fatality rate to 1% (Brook, 2002; Inglesby *et al*, 2002).

Gastrointestinal (GI) anthrax occurs after consuming a large amount of vegetative cells in contaminated raw or undercooked meat (Inglesby *et al*, 2002). Contamination of the food supply by terrorists is a way to cause economic and psychological damages through human exposure to an atypical food borne pathogen (Khan *et al*, 2009). Symptoms include nausea, anorexia, vomiting and fever, then progress to severe abdominal pain and bloody diarrhea. Death results in 2-3 days and is fatal in 25-60% of cases (Brook, 2002; Sirisanthana and Brown, 2002; Fatah *et al*, 2007). Oropharyngeal and abdominal forms of anthrax also occur, where legions grow on the mouth, throat, and stomach of the host. Early detection and treatment of gastrointestinal anthrax is difficult and therefore leads to a high mortality rate.

Anthrax contamination is rare, but has been routinely reported in Africa and Asia (Inglesby *et al*, 2002). Proper cooking and storage conditions can drastically reduce the threat of a possible *B. anthracis* contamination. Khan and colleagues (2009) investigated the survivability of *B. anthracis* spores in processed liquid eggs. They inoculated different preparations of liquid egg with spores and held each sample at a variety of low, moderate, and high temperatures. The study found that spore viability decreased after storage in extreme temperatures, but increase at moderate temperatures. Juneja and colleagues (2010) investigated thermal inactivation of *B. anthracis* spores in irradiated ground beef. Pre-portioned beef patties were inoculated with spores and cooked to an internal temperature of 71.1°C, 82.2°C, or 93.3°C on an open flame grill or a commercial 'clam shell' grill. The study found that cooking to these temperatures lead to a 0.8-3.5 CFU log reduction in spore count. It is important to pass on the information gathered in

these studies to consumers and food handlers, especially in areas where GI Anthrax is common. The effects of proper food storage and cooking must also be emphasized.

Inhalation anthrax is the most severe form of anthrax. Once the spores enter the body, they rapidly germinate, replicate, and release toxins that lead to early symptoms. The incubation period can last from a few days to over one month. Early symptoms include muscle aches, malaise, coughing, headache, fever, and other flu-like symptoms. A brief period of relief may occur before the onslaught of secondary symptoms including respiratory failure, shock, and meningitis (Brook, 2002; Inglesby *et al*, 2002; Fatah *et al*, 2007). Inhalation anthrax is almost always fatal. Non-specific symptoms prevent early diagnosis and administration of antibiotics. An anthrax vaccine is available; however, it is mainly reserved for first responders and military personnel and not the general public. The stability of spores in aerosol form, long incubation period, and inability to quickly begin an antibiotic regimen makes inhalation anthrax one of the most effective forms of biological warfare.

Throughout the 19th Century, the incidence of animal and naturally acquired Anthrax in the United States has declined due to improved animal husbandry and vaccination efforts of 'at risk' populations. After the terrorist attacks of September 11, 2001, Anthrax spores were sent through the mail in the form of a powder to political officials. The spores were manufactured to 'weapons grade', meaning the powder had a high spore concentration, uniform particle size, low electrostatic charge, and were treated to reduce clumping (Inglesby *et al*, 2002). Analysis reported that the powder contained between 100 billion to 1 trillion spores per gram. These attacks lead to 11 confirmed cases of inhalation anthrax, five of whom died. There were also seven confirmed and

four suspected cases of cutaneous anthrax (Brook, 2002; Inglesby *et al*, 2002). After this incident, increased research has gone into Anthrax detection methods.

Novel and Established Detection Methods

Since 2001, research has been done to find ways to distinguish *B. anthracis* from *B. cereus* and other *Bacillus* species. Differentiation can be difficult at low concentrations because of the high degree of DNA homology. This is important because of the vastly different outcomes for the patient and community at large. Kim and colleagues (2005) utilized multiplex real-time PCR and melting curve analysis to detect B. anthracis and the B. cereus group. Primers were designed for the virulence plasmids, pXO1 and pXO2, and *sspE,* a gene coding for spore proteins. Eleven strains of *B. anthracis* and 18 *B. cereus* group strains were analyzed with the assay. The multiplex PCR assay did not produce false positive results from the 29 *B. cereus* groups. All genotypes were detected. The assay was able to detect approximately 500 picograms (10^{-12}) of *B. anthracis* DNA in a sample. Assuming there are three copies of pXO1 and two copies of pXO2, the sensitivity is approximately 83,200 genome copies per PCR reaction (Kim *et al*, 2005). This method is promising considering the small amount of spores needed to cause illness in a patient and the low concentration that can remain in the air after an aerosolized attack.

Hang and colleagues (2008) developed an immunoassay to detect and recover *B. anthracis* spores in environmental samples. Previously, detecting spores at low concentrations was problematic because of cross-contamination between *B. anthracis* antibodies and antibodies for other *Bacillus* species which lead to false positive results. A liquid phase assay was used along with the Integrating Waveguide Biosensor. The

spores were incubated with capture and detection probes prior to analysis. The spores were allowed to germinate and were quantified with PCR. This method allows for detection of 10^3 spores. This low limit of detection is important again because of the low infectious dose and the low concentrations that are found in the environment.

Dauphin and colleagues (2009) evaluated five commercially available nucleic acid extraction kits for their ability to inactivate *B. anthracis* spores. They also compared DNA yields from spores and artificially inoculated environmental samples. This study emphasized the importance of a kill step after the extraction process because of the pathogen's hazardous nature. The kill step also protects the laboratory worker who would likely be handling a large volume of samples in the case of a suspected Anthrax attack. Spores can be hard to work with because of their protective outer shell. Each of the five kits used a different method of detection- ChargeSwitch gDNA Mini Bacteria Kit (magnetic bead technology), Nuclisens Isolation Kit (silica bead technology), Puregene Genomic DNA Purification Kit (precipitation), QIAamp DNA Blood Mini Kit (silica gel spin column), and UltraClean Microbial DNA Isolation Kit (bead beating and silica gel spin column). Sterile cotton swabs and powder samples were inoculated with spore concentrations ranging from 10^7-10^2 CFU/ml. These matrices were chosen to test because they often come into contact with *B. anthracis* spores either as a transport media or sampling tool. The protocol for each kit was followed. PCR analysis was used to test DNA extraction. This study found that the UltraClean kit was most efficient at reducing the viability of spores, with a 5 log reduction in spore viability. PCR results showed that NucliSens, QIAamp, and UltraClean had the lowest limits of detection of spore suspension. They were able to detect 10^3 CFU/ml. ChargeSwitch had the worst limit of

detection at 10^5 CFU/ml. Cost-per-extraction and processing time were also evaluated. This study is important because it objectively evaluated commercial kits and used different types of sample matrices to better simulate real world testing conditions.

Use of gold nanoparticles as reporter in sandwich assay format to detect food borne pathogens

Introduction

Food borne pathogens are a major source of illness and death in the United States and around the world. The inability to attend school or work leads to lost wages and decreased productivity, while hospitalization and treatment leads to rising health care costs. *Salmonella*, *Campylobacter jejuni*, *E. coli O157:H7*, *Listeria monocytogenes*, *Staphylococcus aureus*, and *Clostridium perfringens* are the six major pathogens leading to human illness and death (Tauxe, 2002). It is estimated that each year, food is responsible for 76 million cases of illness in the United States, resulting in 325,000 hospitalizations and 5000 deaths (Mead *et al*, 2000).

Escherichia coli is very common and causes severe stomach cramps and tenderness, watery or bloody diarrhea, nausea and vomiting, and can lead to kidney failure or death in rare but severe cases. Enteritis can also develop in patients with pre-existing conditions (Neal *et al*, 1997). It is of particular concern because it has been linked to recent, multi-state outbreaks in unpasteurized apple juice, ground beef, raw milk, fresh spinach, and prepackaged cookie dough (Olsen *et al*, 2000).

Pathogenic bacteria are transmitted to humans from animal sources or contaminated products (Olsen, 2000). It is important for the safety of the consumer and the reputation of a food company to be able to detect and differentiate viable, pathogenic

bacteria from non-pathogenic bacteria in the complicated matrix of food. These detection methods should be sensitive, rapid, easy to interpret, and inexpensive.

Traditional microbiological methods include media plates and slants. These methods require enrichment steps, purification procedures, lengthy incubation periods, and manual colony counting. The need for enrichment and purification indicate the lack of sensitivity required to directly detect pathogens from a sample (Pyle, 1999). Further steps are required to identify the sub-species or serotype. Selective and differential media is used to distinguish pathogenic *E. coli* from non-pathogenic *E. coli* and other coliforms. The entire process of identification and confirmation can take several days. Although they are time consuming and labor intensive, traditional methods provide definitive and reliable results when performed correctly (Lazcka *et al*, 2007).

The spatial and labor requirements of traditional methods have led to DNA based detection methods. Polymerase chain reaction (PCR) has revolutionized the ability to detect pathogens. However, the DNA from viable and non-viable cells is amplified during PCR and can lead to inflated cell counts. Viable but non-culturable (VBNC) cells are removed through enrichment steps (Olsen, 2000). Amplification of non-virulent bacteria also leads to inflated cell counts when testing for a human pathogen. For example, this is important when testing for *Listeria* species because only one species, *L. monocytogenes*, is a human pathogen. Primers designed specifically for virulence genes will provide accurate amplification of pathogenic bacteria of a particular genus (Olsen, 2000). Naravaneni and Jamil (2004) accomplished this by amplifying the *fimA* gene of *Salmonella* and the *afa* gene of *E. coli*. PCR is a sensitive and rapid technique for

pathogen detection, but food often contains compounds that inhibit amplification. Sample dilution solves this, but lowers sensitivity.

Immunoassays are used to detect pathogens through the use of antibodies. Enzyme-linked immunosorbent assay (ELISA) is a rapid method to detect the presence of an antibody or antigen in a sample. Because the capture structure is immobilized onto a micro-titer plate, the speed of antigen binding is diffusion limited (Stenberg and Nygren, 1988). The use of paramagnetic beads for pathogen detection has recently become popular. These beads are smaller than the pathogen of interest (Pyle, 1999) and are capable of increasing the reaction rate through agitation and increased surface area (Yu and Bruno, 1996).

Paramagnetic beads are often coupled with electrochemiluminescence (ECL). ECL is able to rapidly detect picogram or sub-picogram concentrations of target in a sample (Blackburn *et al*, 1991; Gatto-Menking *et al*, 1995; Yu *et al*, 1995). The free end of the target is tagged with a compound that is capable of producing light after redox cycling. Tripropylamine (TPA) is a cofactor in this reaction. Ruthenium (II) trisbipyridal ($Ru(bpy)_3^{2+}$) is commonly used as a reporter because it is stable and provides high signal-to-background ratios (Yu and Bruno, 1995). Unlike radioisotopic methods, waste materials can be easily disposed of.

ECL detection of the magnetic beads is carried out with a magnet, an electrode, and a detection device. The target-bead hybrids are attracted to the magnet and unbound target is washed away. The electrode is charged, the ruthenium undergoes chemiluminescence, and the detection device records the amount of light given off. Unbound target cannot generate light and therefore reduces background noise (Blackburn

et al, 1991; Yu and Bruno, 1995). This eliminates the need for additional washing steps and aides in the system's sensitivity.

The use of gold nanoparticles (GNP) as a reporter in an assay carried out in the Bioveris M384 Analyzer (IGEN International, Inc, Maryland) was investigated. The GNP will emit energy when the electrode is charged. This energy will be passed to the ruthenium, which in turn will produce more light that ruthenium alone. Ruthenium emits light at 620 nm and the emission wavelength of the GNP depends on their size. Reporter DNA will also be immobilized on the surface of the GNP. The novel GNP reporter is shown in Figure 4.1.

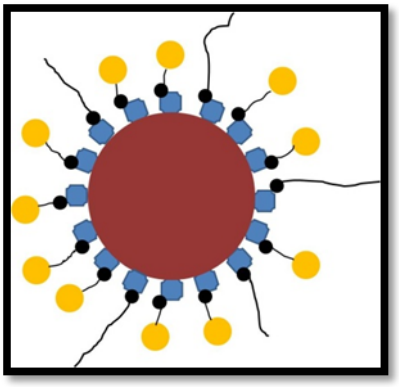

Figure 4.1- Representation of the novel GNP reporter. The GNP is the large red circle, which is coated in streptavidin (blue squares), biotinylated reporter sequence (black circles with black lines), and biotinylated ruthenium (black circles with larger yellow circles). Upon excitation, the GNP will emit energy which will excite the ruthenium. This will have a synergistic effect on the total detectable signal.

This will potentially increase the sensitivity of the assay because multiple copies of target sequence will be attached to the reporter. The signal given off by the GNP reporters will be compared to another reporter consisting of $Ru(bpy)_3^{2+}$ tagged reporter sequence. Paramagnetic beads will be used as the capture probe. The entire 'sandwich' will be attracted to the magnetic electrode and the light will be detected by a photo multiplier tube. The sandwich scheme is shown in Figure 4.2. Unbound reporter probe

and target will be washed away, thereby reducing background noise and eliminating false positives.

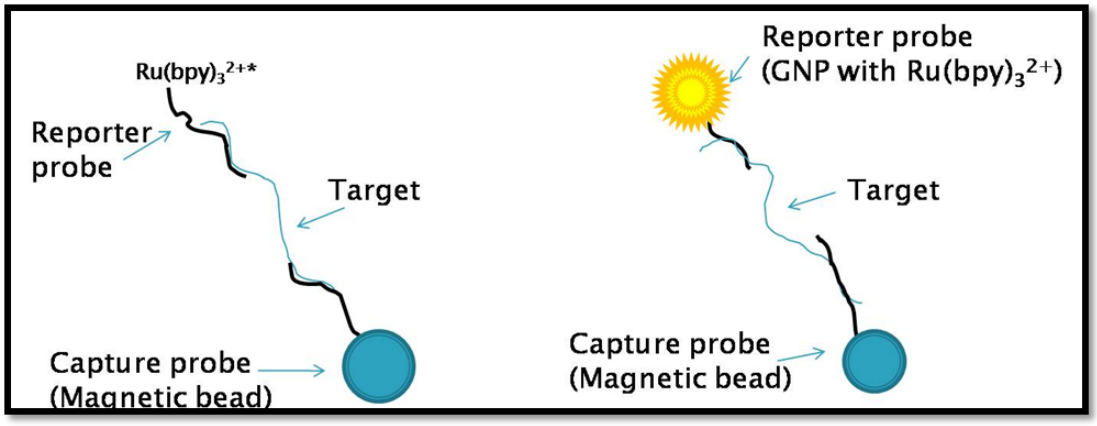

Figure 4.2- Sandwich assay using two different reporters. Both contain a superparamagnetic bead that acts as the capture probe. The bead is bound to an oligonucleotide sequence that is complimentary to one half of the target sequence. On the left, the standard reporter probe is a single strand of the reporter sequence bound to ruthenium. On the right, the novel reporter probe is a GNP bound to several strands of reporter sequence. The reporter sequence is complimentary to the other half of the target sequence. Therefore, the target sequence is sandwiched between the capture and reporter elements.

Materials and Methods

All oligonucleotide sequences were obtained from Eurofins MWG Operon (Alabama) and diluted to the stock concentration according to the package insert. They are similar to sequences found in *E. coli*. Each sequence can be found in Table 4.4.

Table 4.4. List of *E. coli* sequences used in the experiment.

Sequence ID	**5'-3' Sequence**
Reporter 1	Biotin-GGT TGC GCT CGT TGC GGG ACT TAA CCC AAC AT
Reporter 2	Amine-GGT TGC GCT CGT TGC GGG ACT TAA CCC AAC AT
Capture	ACG GTT CCC GAA GGC ACA TTC TCA- Biotin
Target	TGA GAA TGT GCC TTC GGG AAC CGT GAG ACA GGT GCT GCA TGG CTG TCG TCA GCT CGT GTT GTG AAA TGT TGG GTT AAG TCC CGC AAC GAG CGC AACC

Reporter preparation

Biotin-terminated Reporter 1 oligonucleotide was diluted with phosphate buffered saline (PBS; pH 7.5) to a concentration of 250 μmol. The DNA was further diluted to 20 pmol before being added to streptavidin coated gold nanoparticles (Bioassay Works, Maryland). After incubating at room temperature for 45 minutes, there were approximately 10 oligonucleotide strands per GNP. N-hydroxysuccinimide-$Ru(bpy)_3^{2+}$ (NHS-$Ru(bpy)_3^{2+}$; Sigma, Germany) was hydrated with dimethyl sulfoxide (DMSO; Acros Organics, New Jersey) and biotinylated with Amine-PEG_3-Biotin (Thermo, Illinois) and PBS. This was incubated at room temperature for three hours then added to the GNP-oligonucleotide mixture to bind to open streptavidin. The GNPs were run through a 1.5x16 cm column containing Sephadex G-50-80 beads (Sigma, Missouri) to remove free ruthenium from the system and dilute the GNPs. The GNPs were used as collected from the column as the reporter in the sandwich assay.

Amine-terminated Reporter 2 oligonucleotide was diluted to a stock concentration of 100 μM with PBS. NHS-$Ru(bpy)_3^{2+}$ was conjugated to the DNA as described above. Free ruthenium was removed via dialysis in PBS. The reporter was diluted to a final concentration of 0.1 μM with PBS before it was used as a control in the assay.

Capture probe preparation

Superparamagnetic beads (Dynabeads M-280 Streptavidin; Invitrogen, Norway) were used as a capture probe. Double strength (2X) binding and washing buffer (B&W; 10mM Tris, 1mM EDTA, 2M NaCl, pH 7.5) was diluted to single strength (1X) to wash and store the beads until needed. Biotin-terminated capture probe was diluted to a stock concentration of 250 pmol with PBS. Five microliters of capture probe was added to 105

μL PBS before being added to the washed beads. The beads were incubated for 15 minutes at room temperature under gentle shaking and were washed again with 1X B&W buffer. Open streptavidin was filled with $900x10^{-7}$ biotin in PBS. After incubation, the beads were washed and stored in 1X B&W buffer to be used as the capture probe in the assay.

Target preparation

Target oligonucleotide was hydrated with PBS to a stock concentration of 100 μM. The target sequence was further diluted with PBS to a range of 25 fmol/μL to 1500 fmol/μL. PBS (0 fmol/μL) was used as a negative control in the assay.

Assay assembly

The assays were individually assembled in 96-well plates to be read by a Bioveris M384 Analyzer (IGEN International, Inc, Maryland). Each day, quality control and calibration were performed on the instrument according to the manufacturer's instructions to insure accurate and reproducible data. Each well contained 25 μL of capture probe (further diluted 1:20), 100 μL target or PBS, 50 μL reporter probe (GNP or control), and 45 μL hybridization buffer (10X SSC and 60% formamide). Each plate was incubated at room temperature under gentle shaking for 150 minutes. Thirty microliters of PBS was added to each well prior to analysis. The plate was analyzed and data was used to generate a dose response curve of ECL signal vs. target concentration in fmol/μL.

Assay sensitivity was equal to the slope of the linear region of the dose-response curve. Limit of detection (LOD) was calculated by relating the signal from zero target concentration plus three standard deviations to target concentration.

Results

The Bioveris M384 Analyzer was used to detect generic *E. coli* DNA in a sample. Ruthenium-tagged GNPs (Ru-GNP) were used as the experimental reporter in a sandwich assay because they are thought to give a higher signal than the ruthenium-tagged DNA (Ru-DNA) control reporter. Higher signal is linked to a more sensitive assay with a lower limit of detection. Control and experimental assays were run with varying concentrations of target sequence and PBS as a negative control.

Figure 4.3 shows the dose response curves of the GNP reporter and control reporter. Although the linear portion of the graph is small, sensitivity and LOD can still be calculated. The assay using Ru-DNA as a reporter has a LOD of 40 fmol/µL and a sensitivity of 55 fmol/µL, while the assay using Ru-GNP has a LOD of 24 fmol/µL and a sensitivity of 77 fmol/µL. The GNP made a huge improvement in assay performance.

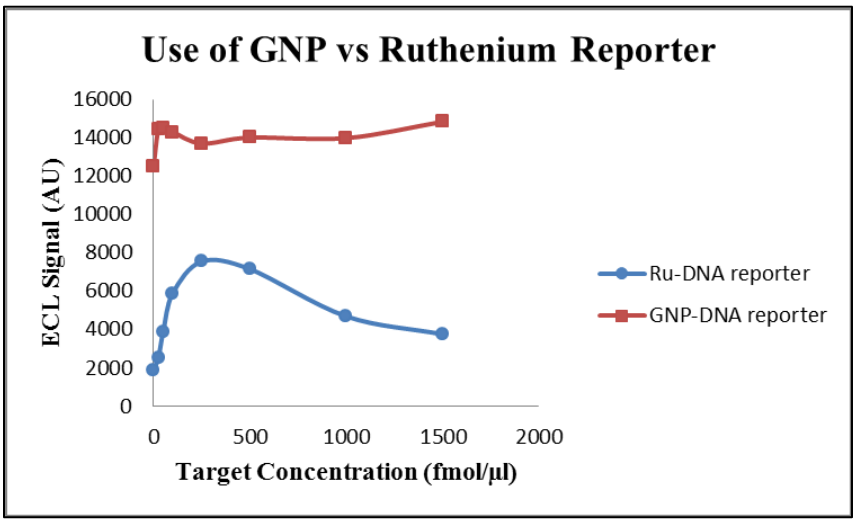

Figure 4.3- Comparison of GNP-DNA and Ru-DNA reporter. The different reporters were used identically in the assay. The GNP reporter had a higher signal, higher sensitivity, and lower limit of detection than the ruthenium reporter.

Discussion

As the global demand for ready to eat meals and minimally processed fresh items increases, the potential for contamination and large scale food borne illness outbreak greatly increases. Traditional microbiological testing methods are accurate, but time consuming and labor intensive. The batch that was produced must wait in the warehouse while samples go out for testing. This reduces plant productivity and costs money, therefore the trend towards rapid methods is becoming increasingly popular.

The reaction mechanism of electrochemiluminescence (ECL) is explained in detail in many sources (Lee *et al,* 2007; Richter, 2004). Briefly, a series of oxidation and reduction reactions occur in sequence to produce an excited state that emits light. The light is detected by a photo multiplier tube and relayed to the user in a numerical value quantified by arbitrary units (AU). A stimulated electrode is needed to start the reaction and tripropylamine (TPA) is a necessary cofactor.

The Bioveris is capable of simultaneously running eight independent ECL reactions. The assay liquid is aspirated into the reaction chamber. As it flows across the electrode, a magnetic force is applied and the superparamagnetic beads, along with target and reporter attached to them, are immobilized. A TPA solution is passed through the chamber, removing unbound target and reporter. The electrode is then stimulated, causing ECL to occur. The signal is detected and a cleaning solution is passed through the chamber, regenerating the electrode surface for the next assay. This scheme is depicted in Figure 4.4.

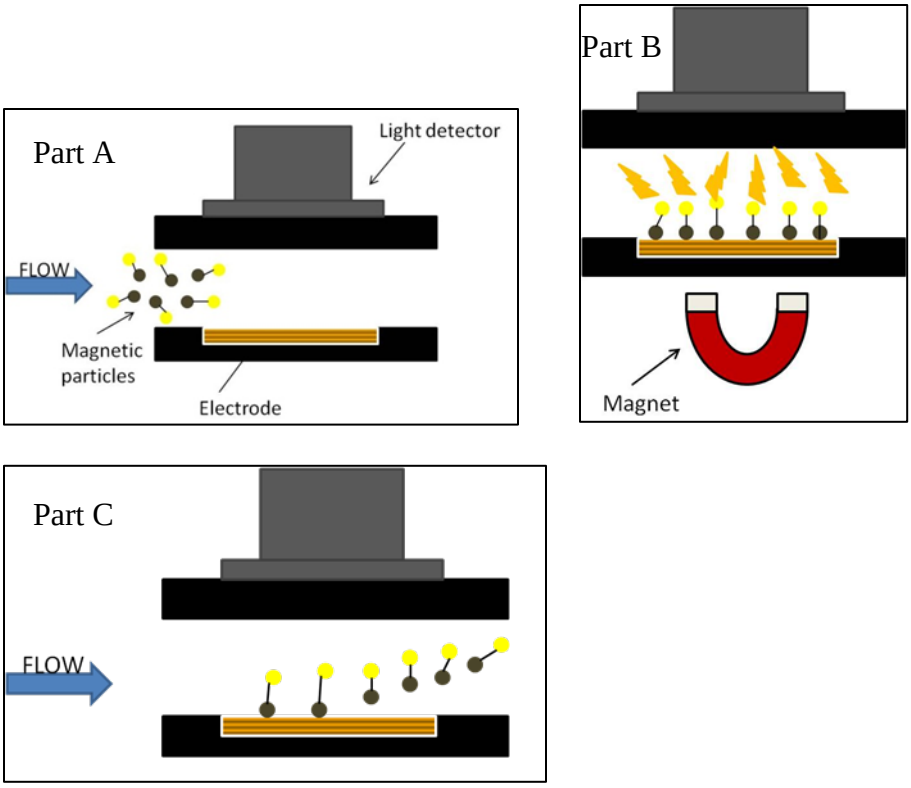

Figure 4.4- Details of the reaction chamber inside the Bioveris M384 Analyzer. Part A shows the capture-reporter complex entering the reaction chamber. Part B shows the magnetic field being applied. The magnetic capture probe is immobilized on the electrode surface and any unbound components are washed away. This decreases background signal. When the electrode is stimulated, light is generated by the bound capture-reporter complex, and is detected by the photomultiplier tube. The data is relayed to the user. Part C shows the capture-reporter complex leaving the reaction chamber. The electrode surface is cleaned and regenerated before the next sample is analyzed.

Traditional methods of pathogen detection can take several days to complete. Using the Bioveris takes only a few hours. Sample preparation, including incubation takes about three hours. Assembling the reporter and capture probes takes about five hours total, but the products can be used for several days. The assay is assembled in a standard 96-well plate and up to 96 samples can be tested at once. Reading a full plate takes about 15 minutes. The Bioveris is equipped to work with a robotic arm to automatically load plates into the instrument. This increases throughput. In the end,

detection time is decreased by several days. This is beneficial as demand for processed food increases.

Using the Ru-GNP reporter in this assay improves assay sensitivity and greatly lowers the LOD. Sensitivity measures the assay's ability to measure small changes in target concentration. The assay using the Ru-GNP is almost three times more sensitive as the Ru-DNA reporter. This could be due to a stronger binding affinity for the target sequence or the ability to capture more target and form large clumps that are joined to the paramagnetic capture probe. Either way, higher signals were generated. The LOD also decreased. Limit of detection (LOD) measures the lowest amount of target concentration that can be detected through background signals. The GNPs have more DNA in an area and are capable of detecting smaller amounts of target in a sample. Adding a greater concentration of Ru-DNA would be ineffective.

Conclusions

Decreasing the amount of time necessary to detect pathogens while lowering LOD and increasing sensitivity is very important. Using the Bioveris M384 Analyzer takes a few short hours. This is rapid compared to the days of intensive work needed for traditional microbiological tests. Sandwich assay format is an easy way to detect target sequences. GNP reporters provide assays with low LOD and high sensitivity. One way to further optimize the assay would be to construct an ECL reader and control all parameters.

BIBLIOGRAPHY

Al-Yousif, Y., Anderson, J., Chard-Bergstrom, C., Kapil, S., 2002. Development, evaluation, and application of lateral-flow immunoassay (immunochromatography) for detection of rotavirus in bovine fecal samples. Clinical and Diagnostic Laboratory Immunology 9,723-724.

Amann, R.I., Binder, B.J., Olson, R.J., Chisholm, S.W., Devereux, R., Stahl, D.A., 1990. Combination of 16S rRNA-targeted oligonucleotide probes with flow cytometry for analyzing mixed microbial populations. Applied and Environmental Microbiology 56, 1919-1925.

Amann, R., Ludwig, W., 2000. Ribosomal RNA-targeted nucleic acid probes for studies in microbial ecology. FEMS Microbiological Reviews 24, 555-565.

Baeumner, A.J., Pretz, J., Fang, S., 2004. A universal nucleic acid sequence biosensor with nanomolar detection limits. Analytical Chemistry 76, 888-894.

Bhalla, D.K., Warheit, D.B., 2004. Biological agents with potential for misuse: a historical perspective and defensive measures. Toxicology and Applied Pharmacology 199, 71-84.

Biegala, I.C., Cuttle, M., Mary, I., Zubkov, M., 2005. Hybridization of picoeukaryotes by eubacterial probes is widespread in the marine environment. Aquatic Microbial Ecology 41, 293-297.

Biermann, T., Schwarze, B., Zedler, B., Betz, P., 2004. On-site testing of illicit drugs: The use of the drug-testing device “Toxiquick®”. Forensic Science International 143, 21-25.

Blackburn, G.F., Shah, H.P., Kenten, J.H., Leland, J., Kamin, R.A., Link, J., Peterman, J., Powell, M.J., Shah, A., Talley, D.B., 1991. Electrochemiluminescence detection for development of immunoassays and DNA probe assays for clinical diagnosis. Clinical Chemistry 37, 1534-1539.

Blencowe, T., Pehrsson, A., Lillsunde, P., Vimpari, K., Houwing, Smink, B., Mathijssen, R., Van der Linde, T., Legrand, S-A., Pil, K., Verstraete, A., 2011. An analytical evaluation of eight on-site oral fluid drug screening devices using laboratory confirmation results from oral fluid. Forensic Science International 208, 173-179

Bochdansky, A.B., Huang, L., 2010. Re-evaluation of the EUK516 probe for the domain eukarya results in a suitable probe for the detection of kinetoplastids, an important Group of parasitic and free-living flagellates. Journal of Eukaryotic Microbiology 57, 229-235.

Brook, I., 2002. The prophylaxis and treatment of anthrax. International Journal of Antimicrobial Agents 20, 320-325.

Butler, S.A., Khanlian, S.A., Cole, L.A., 2001. Detection of early pregnancy forms of human chorionic gonadotropin by home pregnancy test devices. Clinical Chemistry 47, 2131-2136.

Carter, D.J., Cary, R.B., 2007. Lateral flow microarrays: a novel platform for rapid nucleic acid detection based on miniaturized lateral flow chromatography. Nucleic Acids Research, 35, 1-11.

Chang, Z., Zhou, J., Zhao, K., Zhu, N., He, P., Fang, Y., 2006. $Ru(bpy)_3^{2+}$-doped silica nanoparticle DNA probe for the electrogenerated chemiluminescence detection of DNA hybridization. Electrochimica Acta 52, 575-580.

Corstjens, P., Zuiderwijk, M., Nilsson, M., Feindt, H., Niedbala, R.S., Tanke, H.J., 2003. Lateral-flow and up-converting phosphor reporters to detect single-stranded nucleic acids in a sandwich-hybridization assay. Analytical Biochemistry 312, 191-200.

Danzig, R., Berkowsky, P.B., 1997. Why should we be concerned about biological warfare?. Journal of the American Medical Association 278, 431-432.

Dauphin, L.A., Moser, B.D., Bowen, M.D., 2009. Evaluation of five commercial nucleic acid extraction kits for their ability to inactivate Bacillus anthracis spores and comparison of DNA yields from spores and spiked environmental samples. Journal of Microbiological Methods 76, 30-37.

Edwards, K.A., Baeumner, A.J., 2006. Optimization of DNA-tagged dye-encapsulated liposomes for lateral-flow assays based on sandwich hybridization. Analytical and Bioanalytical Chemistry 286, 1335-1343.

Ertner, R.A., Gates, S.I., Waagner, D.C., Kaye, A.D., 2003. Smallpox and plague as agents of bioterrorism. Seminars in Anesthesia, Perioperative Medicine and Pain 22, 247-257.

Esch, M.B., Baeumner, A.J., Durst, R.A., 2001. Detection of *Cryptosporidium parvum* using oligonucleotide-tagged liposomes in a competitive assay format. Analytical Chemistry 73, 3162-3167.

Fatah, A.A., Arciles, R.D., Chekol, T., Lattin, C.H., Sadik, O.A., Aluoch, A., 2007. Guide for the Selection of Biological Agent Detection Equipment for Emergency First Responders, 2nd Edition *United States Department of Homeland Security*

Fleet, F.H., 2011. Yeast Spoilage of Foods and Beverages. In: Kurtzman, C.P., Fell, J.W., Boekhout, T, (Eds.), The Yeasts: A Taxonomic Study, Volume 1. Elsevier, London, pp. 53-62.

Fuchs, B.M., Wallner, G., Beisker, W., Schwippl, I., Ludwig, W., Amann, R., 1998. Flow cytometric analysis of the in situ accessibility of *Escherichia coli* 16S rRNA for fluorescently labeled oligonucleotide probes. Applied and Environmental Microbiology 66, 4973-4982.

Fuchs, B.M., Syutsubo, K., Ludwig, W., Amann, R., 2001. In situ accessibility of Escherichia coli 23S rRNA to fluorescently labeled oligonucleotide probes. Applied and Environmental Microbiology 67, 961-968.

Gatto-Manking, D.L., Yu, H., Bruno, J.G., Goode, M.T., Miller, M., Zulich, A.W., 1995. Sensitive detection of biotoxoids and bacterial spores using an immunomagnetic electrocheminescence sensor. Biosensors and Bioelectronics 10, 501-507.

Gessler, F., Pagel-Wieder, S., Avondet, M-A., Böhnel, H., 2007. Evaluation of lateral flow assays for the detection of botulinum neurotoxin type A and their application in laboratory diagnosis of botulism. Diagnostic Microbiology and Infectious Disease 57, 243-249.

Giovannoni, S.J., DeLong, E.F., Olsen, G.J., Pace, N.R., 1988. Phylogenetic group-specific oligodeoxynucleotide probes for identification of single microbial cells. Journal of Bacteriology 170, 720-726.

Gooding, J.J., 2006. Biosensor technology for detecting biological warfare agents: Recent progress and future trends. Analytica Chimica Acta 559, 137-151.

Gougouli, M., Kalantzi, K., Beletsiotis, E., Koutsoumanis, P., 2011. Development and application of predictive models for fungal growth as tools to improve quality in yogurt production. Food Microbiology 28, 1453-1462.

Granum, P.E., 2005. Bacillus cereus. In: Fratamino, P.M., Bhunia, A.K., Smith, J.L. (Eds.), Foodborne Pathogens: Microbiology and Molecular Biology. Horizon Scientific Press, Norwich, pp. 409-417.

Grigg, B., Modeland, V., 1989. The cyanide scare; a tale of two grapes. FDA Consumer 23, 7-11.

Hang, J., Sundaram, A.K., Zhu, P., Shelton, D.R., Karns, J.S., Martin, P.A.W., Amstutz, P., Tang, C-M., 2008. Development of a rapid and sensitive immunoassay for detection and subsequent recovery of Bacillus anthracis spores in environmental samples. Journal of Microbiological Methods 73, 242-246.

Howarter, J.A., Youngblood, J.P., 2006. Optimization of silica silanization by 3-aminopropyltriethoxysilane. Langmuir 22, 11142-11147.

Inácio, J., Behrens, S., Fuchs, B.M., Fonseca, A., Spencer-Martins, I., Amann, R., 2003. In situ accessibility of *Saccharomyces cerevisiae* 26S rRNA to Cy3-labeled oligonucleotide probes comprising the D1 and D2 domains. Applied and Environmental Microbiology 69, 2899-2905.

Inglesby, T.V., Dennis, D.T., Henderson, D.A., Bartlett, J.G., Ascher, M.S., Eitzen, E., Fine, A.D., Friedlander, A.M., Hauer, J., Koerner, J.F., Layton, M., McDade, J., Osterholm, M.T., O'Toole, T., Parker, G., Perl, T.M., Russell, P.K., Schoch-Spana, M., Tonat, K., 2000. Plague as a biological weapon. Journal of the American Medical Association 283, 2281-2290.

Inglesby, T.V., O'Toole, T., Henderson, D.A., Bartlett, J.G., Ascher, M.S., Eitzen, E., Friedlander, A.M., Gerberding, J., Hauer, J., Hughes, J., 2002. Anthrax as a biological weapon, 2002: updated recommendations for management. Journal of the American Medical Association 287, 2236.

Jakobsen, M., Narvhus, J., 1996. Yeasts and their possible beneficial and negative effects on the quality of dairy products. International Dairy Journal 6, 755-768.

Jasson, V., Jacxsens, L., Luning, P., Rajkovic, A., Uyttendaele, M., 2010. Alternative microbial methods: an overview and selection criteria. Food Microbiology 27, 710-730.

Juneja, V.K., Porto-Fett, C.S., Call, J.E., Marks, H.B., Tamplin, M.L., Luchansky, J.B., 2010. Thermal inactivation of Bacillus anthracis Sterne in irradiated ground beef heated in a water bath or cooked on commercial grills. Innovative Food Science and Emerging Technologies 11, 123-129.

Khan, S.A., Sung, K., Nawaz, M.S., Cerniglia, C.E., Tamplin, M.L., Phillips, R.W., Kelley, L.C., 2009. The survivability of Bacillus anthracis (Sterne strain) in processed liquid eggs. Food Microbiology 26, 123-127.

Kim, K., Seo, J., Wheeler, K., Park, C., Kim, D., Park, S., Kim, W., Chung, S-I., Leighton, T., 2005. Rapid genotypic detection of Bacillus anthracis and the Bacillus cereus group by multiplex PCR melting curve analysis. FEMS Immunological and Medical Microbiology 42, 301-310.

Koehler, T.M. 2009. Bacillus anthracis physiology and genetics. Molecular Aspects of Medicine 30, 386-396.

Koets, M., Sander, I., Bogdanovic, J., Doekes, G., van Amerongen, A., 2006. A rapid lateral flow immunoassay for the detection of fungal alpha-amylase at the workplace. Journal of Environmental Monitoring 8, 942-946.

Kolavic, S.A., Kimura, A., Simons, S.L., Slutsker, L., Barth, S., Haley, C.E., 1997. An outbreak of *Shigella dysenteriae* Type 2 among laboratory workers due to intentional food contamination. Journal of the American Medical Association 278, 396-398.

Kosse, D., Seiler, H., Amann, R., Ludwig, W., Scherer, S., 1997. Identification of yoghurt-spoiling yeasts with 18S rRNA-targeted oligonucleotide probes. Systematic and Applied Microbiology 20, 468-480.

Kuritza, A., Salyers, A., 1985. Use of a species-specific DNA hybridization probe for enumerating *Bacteroides vulgatus* in human feces. Applied and Environmental Microbiology 50, 958-964.

Kwakye, S., Baeumner, A., 2003. A microfluidic biosensor based on nucleic acid sequence recognition. Analytical and Bioanalytical Chemistry 376, 1062-1068.

Lane, D.J., Pace, F., Olsen, G.J., Stahl, D.A., Sogin, M.L., Pace, N.R., 1985. Rapid determination of 16S rRNA sequences for phylogenetic analyses. Proceedings of the National Academy of Sciences of the United States of America 82, 6955-6959.

Lazcha, O., Del Campo, F.J., Muñoz, F.X., 2007. Pathogen detection: a perspective of traditional methods and biosensors. Biosensors and Bioelectronics 22, 1205-1217.

Lee, J.G., Yun, K., Lim, G.S., Lee, S.E., Kim, S., Park, J.K., 2007. DNA biosensor based on the electrochemiluminescence of $Ru(bpy)_3^{2+}$ with DNA-binding intercalators. Biochemistry 70, 228-234.

Leung, W., Chan, C.P.Y., Bosgoed, F., Lehmann, K., Renneberg, I., Lehmann, M., Renneberg, R., 2003. One-step quantitative cortisol dipstick with proportional reading. Journal of Immunological Methods 281, 109-118.

Lischewski, A., Amann, R.I., Harmsen, D., Merkert, H., Hacker, J., Morschhäuser, J., 1996. Specific detection of *Candida albicans* and *Candida tropicalis* by fluorescent *in situ* hybridization with an 18S rRNA-targeted oligonucleotide probe. Microbiology 142, 2731-2740.

Mabey, D., Peeling, R.W., Ustianowski, A., Perkins, M.D., 2004. Diagnostics for the developing world. Microbiology 2, 231-240.

Mao, X., Ma, Y., Zhang, A., Zhang, L., Zeng, L., Lu, G., 2009. Disposable nucleic acid biosensors based on gold nanoparticle probes and lateral flow strips. Analytical Chemistry 81, 1660-1668.

Mataragas, M., Dimitriou, V., Skandamis, P.N., Drosinos, E.H., 2011. Quantifying the spoilage and shelf-life of yoghurt with fruits. Food Microbiology 28, 611-616.

Mead, P.S., Slutsker, L., Dietz, V., McCaig, L.F., Bresee, J.S., Sapiro, C., Griffin, P.M., Tauxe, R.V., 2000. Food-related illness and death in the United States. Journal of Environmental Health 62, 9-18.

Meyer, M.H.F., Stehr, M., Bhuju, S., Krause, H.J., Hartman, M., Miethe, P., Singh, M., Keusgen, M., 2007. Magnetic biosensor for the detection of *Yersinia pestis*. Journal of Microbiological Methods 68, 218-224.

Muhammad-Tahir, Z., Alocilja, E.C., 2004. A disposable biosensor for pathogen detection in fresh produce samples. Biosystems Engineering 88, 145-151.

Naravaneni, R., Jamil, K., 2005. Rapid detection of food-borne pathogens by using molecular techniques. Journal of Medical Microbiology 54, 51-54.

Neal, K.R., Hebden, J., Spiller, R., 1997. Prevalence of gastrointestinal symptoms six months after bacterial gastroenteritis and risk for development of the irritable bowel syndrome: postal survey of patients. British Medical Journal 314, 779.

Nobs, L., Buchegger, F., Gurny, R., Allémann, E., 2004. Current methods for attaching targeting ligands to liposomes and nanoparticles. Journal of Pharmaceutical Sciences 93, 1980-1992.

Nugen, S.R., Baeumner, A.J., 2008. Trends and opportunities in food pathogen detection. Analytical and Bioanalytical Chemistry 391, 451-454.

Oku, Y., Kamiya, K., Kamiya, H., Shibahara, Y., Ii, T., Uesaka, Y., 2001. Development of oligonucleotide lateral-flow immunoassay for multi-parameter detection. Journal of Immunological Methods 258, 73-84.

Olsen, J.E., 2000. DNA-based methods for detection of food-borne bacterial pathogens. Food Research International 33, 257-266.

Olsen, S.J., MacKinon, L.C., Goulding, J.S., Bean, N.H., Slutsker, L., 2000. Surveillance for foodborne disease outbreaks- United States, 1993-1997. MMWR Surveillance Summaries 49, 1-51.

Ow, H., Larson, D.R., Srivastava, M., Baird, B.A., Webb, M.W., Wiesner, U., 2005. Bright and stable core-shell fluorescent silica nanoparticles. Nano Letters 5, 113-117.

Posthuma-Trumpie, G.A., Korf, J., van Amerongen, A., 2009. Lateral flow (immuno)assay: its strengths, weaknesses, opportunities, and threats. A literature survey. Analytical and Bioanalytical Chemistry 393, 569-582.

Pyle, B.H., Broadway, S.C., McFeters, G.A., 1999. Sensitive detection of *Escherichia coli* O157:H7 in food and water by immunomagnetic separation and solid-phase laser cytometry. Applied and Environmental Microbiology 65, 1966-1972.

Richter, M.R., 2004. Electrochemiluminescene (ECL). Chemical Reviews 104, 3003-3036.

Rong-Hwa, S., Shiao-Shek, T., Der-Jiang, C., Yao-Wen, H., 2010. Gold nanoparticle-based lateral flow assay for detection of staphylococcal enterotoxin B. Food Chemistry 118, 462-466.

Rossi, L.M., Shi, L., Quina, F.H., Rosenzweig, Z., 2005. Stöber synthesis of monodispersed luminescent silica nanoparticles for bioanalytical assays. Langmuir 21, 4277-4280.

Santra, S., Wang, K., Tapec, R., Tan, W., 2001a. Development of novel dye-doped silica nanoparticles for biomarker application. Journal of Biomedical Optics 6, 160-166.

Santra, S., Zhang, P., Wang, K., Tapec, R., Tan, W., 2001b. Conjugation of biomolecules with luminophore-doped silica nanoparticles for photostable biomarkers. Analytical Chemistry 73, 4988-4993.

Sirisanthana, T., Brown, A.E., 2002. Anthrax of the gastrointestinal tract. Emerging Infectious Diseases 8, 649-651.

Skottrup, P.D., Nicolaisen, M., Justesen, A.F., 2008. Towards on-site pathogen detection using antibody-based sensors. Biosensors and Bioelectronics 24, 339-348.

Smith, P.K., Krohn, R.I., Hermanson, G.T., Mallia, A.K., Gartner, F.H., Provenzano, M.D., Fujimoto, E.K., Goeke, N.M., Olsen, B.J., Klenk, D.C., 1985. Measurement of protein using bicinchoninic acid. Analytical Biochemistry 150, 76-85.

Smith, J.E., Wang, L., Tan, W., 2006. Bioconjugated silica-coated nanoparticles for bioseparation and bioanalysis. Trends in Analytical Chemistry 25, 848-855.

Soukoulis, C., Panagiotidis, P., Kourell, R., Tzia, C., 2007. Industrial yogurt manufacture: monitoring of fermentation process and improvement of final product quality. Journal of Dairy Science 90, 2641-2654.

Stenberg, M., Nygren, H., 1988. Kinetics of antigen-antibody reactions at solid-liquid interface. Journal of Immunological Methods 113, 3-15.

Stöber, W., Fink, A., Bohn, E., 1968. Controlled growth of monodisperse silica spheres in the micron size range. Journal of Colloid and Interface Science 26, 62-69.

Tapec, R., Zhao, X.J., Tan, W., 2002. Development of organic dye-doped silica nanoparticles for bioanalysis and biosensors. Journal of Nanoscience and Nanotechnology 2, 405-409.

Tauxe, R.V., 2002. Emerging foodborne pathogens. International Journal of Food Microbiology 78, 31-41.

Török, T.J., Tauxe, R.V., Wise, R.P., Livengood, J.R., Sokolow, R., Mauvais, S., Birkness, K.A., Skeels, M.R., Horan, J.M., Foster, L.R., 1997. A large community outbreak of salmonellosis caused by intentional contamination of restaurant salad bars. Journal of the American Medical Association 278, 389-395.

Vandenberg, E., Elwing, H., Askendal, A., 1991. Protein immobilization to 3-aminopropyl triethoxy silane/glutaradehyde surface: characterization by detergent washing. Journal of Colloid and Interface Science 143, 327-335.

Velusamy, V., Arshak, K., Korostynska, O., Oliwa, K., Adley, C., 2010. An overview of foodborne pathogen detection: in the perspective of biosensors. Biotechnology Advances 28, 232-254.

Viljoen, B.C., Lourens-Hattingh, A., Ikalafeng, B., Peter, G., 2003. Temperature abuse initiating yeast growth in yoghurt. Food Research International 36, 193-197.

Volkov, A., Mauk, M., Corstjens, P., Niedbala, R.S., 2009. Rapid Prototyping of Lateral Flow Assays. In: Rasooly, A., Gerold, K.E. (Eds.), Methods in Molecular Biology: Biosensors and Biodetection, Vol. 504. Humana Press, Clifton, pp. 217-235.

Wang, S., Zhang, C., Wang, J., Zhang, Y., 2005. Development of colloidal gold-based flow-through and lateral-flow immunoassays for the rapid detection of the insecticide carbaryl. Analytica Chimica Acta 546, 161-166.

Woese, C.R., 1987. Bacterial evolution. Microbiological Reviews 51, 221-271.

Whittaker, P., 2009. Comparison of *Yersinia pestis* to other closely related *Yersinia* species using fatty acid profiles. Food Chemistry 116, 629-632.

Xu, Q.F., Xu, H., Gu, H., Li, J.B., Wang, Y., Wei, M., 2009. Development of lateral flow immunoassay system based on superparamagnetic nanobeads as labels for rapid quantitative detection of cardiac troponin I. Material Science and Engineering C 29,702-707.

Yan, Z., Zhou, L., Zhao, Y., Wang, J., Huang, L., Hu, K., Liu, H., Wang, H., Guo, Z., Song, Y., Huang, J., Yang, R., 2006. Rapid quantitative detection of *Yersinia pestis* by lateral-flow immunoassay and up-converting phosphor technology-based biosensor. Sensors and Actuators B 119, 656-663.

Yang, M., Kostov, Y., Bruck, H.A., Rasooly, A., 2009. Gold nanoparticle-based enhanced chemiluminescence immunosensor for detection of Staphylococcal Enterotoxin B (SEB) in food. International Journal of Food Microbiology 133, 265-271.

Yu, H., Bruno, J.G., Cheng, T., Calomiris, J.J., Goode, M.T., Gatto-Menking, D.L., 1995. A comparative study of PCR product detection a quantitation by electrochemiluminescence and fluorescence. Luminescence 10, 239-245.

Yu, H., Bruno, J.G., 1996. Immunomagnetic-electrochemiluminescent detection of *Escherichia coli* O157 and *Salmonella typhimurium* in foods and environmental water samples. Applied and Environmental Microbiology 62, 587-592.

Zaytseva, N.V., Goral, V.N., Montagna, R.A., Baeumner, A.J., 2005. Development of a microfluidic biosensor module for pathogen detection. Lab on a Chip 5, 805-811.

Zhang, Q., Huang, R., Guo, L.H., 2009. One-step and high-density protein immobilization on epoxysilane-modified silica nanoparticles. Chinese Science Bulletin 54, 2620-2626.

Zhao, X., Tapec-Dytioco, R., Tan, W., 2003. Ultrasensitive DNA detection using highly fluorescent bioconjugated nanoparticles. JACS Communications 125, 11474-11475.

Zhao, X., Pierce, D.T., Huan, Y., 2010. A Sensitive Sandwich DNA Array Using Fluorescent Nanoparticle Probes. In: Minteer, S.D. (Ed.), Methods in Molecular Biology, vol. 321: Microfluidic Techniques: Reviews and Protocols. Human Press Inc., Totowa, pp. 141-155.